Event-Triggered Robust Stabilization of Nonlinear Input-Constrained Systems Using Single Network Adaptive Critic Designs

Xiong Yang and Haibo He, *Fellow, IEEE*

***Abstract*—In this paper, we study the event-triggered robust stabilization problem of nonlinear systems subject to mismatched perturbations and input constraints. First, with the introduction of an infinite-horizon cost function for the auxiliary system, we transform the robust stabilization problem into a constrained optimal control problem. Then, we prove that the solution of the event-triggered Hamilton–Jacobi–Bellman (ETHJB) equation, which arises in the constrained optimal control problem, guarantees original system states to be uniformly ultimately bounded (UUB). To solve the ETHJB equation, we present a single network adaptive critic design (SN-ACD). The critic network used in the SN-ACD is tuned through the gradient descent method. By using Lyapunov method, we demonstrate that all the signals in the closed-loop auxiliary system are UUB. Finally, we provide two examples, including the pendulum system, to validate the proposed event-triggered control strategy.**

***Index Terms*—Adaptive critic designs (ACDs), adaptive dynamic programming (ADP), event-triggered control (ETC), input constraints, neural network (NN), reinforcement learning (RL).**

I. Introduction

Adaptive critic designs (ACDs) have emerged as effective tools to solve optimal control problems over the past several decades [1]–[3]. The typical structure applied to implement ACDs is the actor-critic architecture, where the actor performs a control policy to environment (or controlled systems), and the critic offers an estimation of the value of that control policy and gives feedback information to the actor. In the computational intelligence community, adaptive dynamic programming (ADP) [4] and reinforcement learning (RL) [5] are nearly in the same spirits as ACDs (e.g., all of them have similar implementation architectures). Thus, they are often regarded as synonyms for ACDs. In this paper, we view ADP and RL as a kind of ACDs. The early contributors to ADP and RL included Werbos [6] and Sutton and Barto [7]. After that, many scholars showed their interest in ADP and RL. Thus, all kinds of ADP and RL methods were developed, such as local value/policy iterative ADP [8], [9], goal representation ADP [10], robust ADP [11], [12], single network ACDs (SN-ACDs) [13], online RL [14], [15], off-policy RL [16], and manifold RL [17].

In recent years, applications of ACDs to study robust stabilization problems have been extensively reported [18]–[22]. In the existing literature, the robust controllers for nonlinear systems are generally obtained by solving H_∞ optimal control problems or nonlinear zero-sum games under the framework of ACDs. Nevertheless, a limitation of solving H_∞ optimal control problems or zero-sum games is that one needs to make sure the existence of saddle points. Unfortunately, it is challengeable to judge whether the saddle point of nonlinear systems exists or not. To avoid this difficulty, Lin and Brandt [23] introduced an indirect method, which aimed at converting the robust control problem into an H_2 optimal control problem. Then, one was able to derive the robust controller for nonlinear systems by solving the H_2 optimal control problem. Recently, the indirect method together with ACDs was proposed by Adhyaru *et al.* [24] to design the robust controller for uncertain nonlinear input-constrained systems. After that, Mu *et al.* [25] used the indirect method and ACDs together to derive a robust tracking control strategy for nonlinear systems subject to matched uncertainties. By using a similar method as [25], Qu *et al.* [26] obtained a decentralized tracking control of large-scale nonlinear systems with matched interconnections. An important difference between [25] and [26] was that [26] did not require the initial admissible control while implementing the proposed robust control scheme. Later, Zhang *et al.* [27] extended the work of [26] to design an optimal guaranteed cost sliding mode controller for constrained nonlinear systems with matched/mismatched disturbances. In all the above mentioned literature, the robust control strategies were implemented in the time-triggering mechanism. In other words, the robust control schemes were implemented periodically. According to [28], the time-triggered control schemes often had difficulties in handling the control problems with the conditions that there were only finite computation bandwidths as well as the limited communication resources.

To overcome these difficulties, many event-triggered control (ETC) approaches have been introduced [29]–[32]. Unlike

Manuscript received April 4, 2018; accepted June 29, 2018. This work was supported in part by the National Natural Science Foundation of China under Grant 61503379, in part by the China Scholarship Council under the State Scholarship Fund, and in part by the National Science Foundation under Grant CMMI 1526835 and Grant ECCS 1731672. This paper was recommended by Associate Editor Z. Wang. *(Corresponding author: Haibo He.)*

X. Yang is with the School of Electrical and Information Engineering, Tianjin University, Tianjin 300072, China (e-mail: xiong.yang@tju.edu.cn).

H. He is with the Department of Electrical, Computer and Biomedical Engineering, University of Rhode Island, Kingston, RI 02881 USA (e-mail: haibohe@uri.edu).

Color versions of one or more of the figures in this paper are available online at http://ieeexplore.ieee.org.

Digital Object Identifier 10.1109/TSMC.2018.2853089

the time-triggered controller, the event-triggered controller is updated aperiodically. Specifically, the event-triggered controller is updated only when the deviation between the system state and the desired value crosses a prescribed threshold. Due to this characteristic, the ETC strategies can overcome the shortcomings of the time-triggered control schemes [28]. Thus, many studies on robust ETC methods were reported. Wang *et al.* [33] presented an event-based robust controller for uncertain nonlinear systems via the SN-ACD. After that, with the combination of the SN-ACD and the concurrent learning technique, Zhang *et al.* [34] developed a robust ETC of nonlinear systems with mismatched disturbances. Compared with [33], Zhang *et al.* [34] relaxed the persistence of excitation (PE) condition. Recently, by applying ACDs to solve the event-triggered H_∞ optimal control problems, Mu *et al.* [35] and Zhang *et al.* [36] obtained robust ETC strategies for nonlinear systems, respectively. Owing to the existence of the aforementioned limitation in solving H_∞ optimal control problems, these robust ETC schemes usually encountered difficulties in engineering applications. On the other hand, due to physical characteristics of actuators in engineering industries, it is necessary to take actuator saturations (i.e., input constraints) into account. To address this problem, Wang *et al.* [37] studied the constrained robust ETC problem of nonlinear input-affine systems with *matched* uncertainties using ACDs. However, to the best of our knowledge, there are few studies developing the robust ETC scheme for nonlinear input-constrained systems subject to *mismatched* perturbations, especially without using the H_∞ control theory [38]. This motivates this paper.

In this paper, a robust ETC strategy is developed for nonlinear input-constrained systems with mismatched perturbations. First, by constructing an infinite-horizon cost function for the auxiliary system, the robust stabilization problem is converted into a constrained optimal control problem. Then, it is proved that the solution of the event-triggered Hamilton–Jacobi–Bellman (ETHJB) equation, arising in the constrained optimal control problem, keeps original system states uniformly ultimately bounded (UUB). To solve the ETHJB equation, the SN-ACD is proposed. The critic network used in the SN-ACD is updated by using the gradient descent method. Finally, uniform ultimate boundedness of all the signals in the closed-loop auxiliary system is demonstrated via Lyapunov method.

The novelties of this paper include three aspects.

1) Different from [34] updating the augmented control in an mechanism regarded as the combination of time-triggering and event-triggering mechanisms (ETMs), this paper tunes the augmented control only in the ETM. Hence, the developed control scheme has an advantage in decreasing the computational burden.
2) Unlike [35] and [36] solving the event-triggered H_∞ optimal control problems, this paper obtains the robust ETC via an indirect method. Thus, the present method relaxes the requirement of judging the existence of the saddle point, which is an indispensable procedure in solving H_∞ optimal control problems.
3) This paper extends the work of [37] to develop a robust ETC strategy for nonlinear input-constrained systems with *mismatched* perturbations. Generally, robust control methods for nonlinear systems with *matched* disturbances are not applicable to those systems with *mismatched* disturbances (*note:* the definitions of systems with *mismatch* disturbances and systems with *match* disturbances can refer to [23]). Furthermore, when considering input constraints, it increases the difficulty in making such an extension.

It is worth emphasizing here that the knowledge of system dynamics [i.e., $f(x)$ and $g(x)$ in system (1) (*note:* see Section II-A)] is required to be known. Actually, by using a similar fuzzy technique proposed in [39], this condition can be removed. For simplicity, in this paper we assume that the information of system dynamics is available.

The rest of this paper is structured as follows. After briefly presenting problem descriptions and preliminaries in Section II, we propose the robust ETC scheme in Section III. Then, after discussing the stability analysis in Section IV, we provide two examples to validate the established theoretical results in Section V. Finally, several concluding remarks and future works are given in Section VI.

Notation: $\mathbb{R}$, $\mathbb{N}$, and $\mathbb{N}^+$ denote the sets of real numbers, non-negative integers, and positive integers, respectively. $\mathbb{R}^m$ and $\mathbb{R}^{n\times m}$ denote the spaces of real m-vectors and $n \times m$ real matrices, respectively. I_n is the identity matrix of dimension $n \times n$. T is the transposition symbol. $\|\alpha\| = \sqrt{\sum_{i=1}^{n} |\alpha_i|^2}$ is the Euclidean norm of the vector $\alpha = (\alpha_1, \alpha_2, \ldots, \alpha_n)^\mathsf{T} \in \mathbb{R}^n$. Ω is a subset of $\mathbb{R}^n$, i.e., $\Omega \subset \mathbb{R}^n$. $\|A\|$ denotes the Frobenius-norm of the matrix $A \in \mathbb{R}^{n\times m}$. $V_x^* = \partial V^*(x)/\partial x$ is the partial derivative of $V^*(x)$ with respect to $x \in \mathbb{R}^n$.

II. Problem Description and Preliminaries

A. Problem Description

Consider the continuous-time nonlinear system with a mismatched perturbation given in the form

$$\dot{x}(t) = f(x(t)) + g(x(t))u(t) + k(x(t))d(x(t)) \tag{1}$$

where $x(t) \in \mathbb{R}^n$ is the state, $u(t) \in \mathfrak{U}$ is the control input, $\mathfrak{U} = \{(u_1, u_2, \ldots, u_m) \in \mathbb{R}^m : |u_i| \leq \beta, i = 1, 2, \ldots, m\}$, $\beta > 0$ is the upper bound, $f(x) \in \mathbb{R}^n$, $g(x) \in \mathbb{R}^{n\times m}$, and $k(x) \in \mathbb{R}^{n\times p}$ (*note:* $k(x) \neq g(x)$ when $p = m$) are known smooth functions, and $d(x) \in \mathbb{R}^p$ is an *uncertain* perturbation. Here, $x_0 = x(0)$ is the initial state.

Assumption 1: System (1) is controllable. Meanwhile, $x = 0$ is the equilibrium point of system (1) when letting $u(t) = 0$ and $d(x(t)) = 0$ for all $t \geq 0$.

Assumption 2: The control matrix $g(x)$ is bounded as $0 < g(x) \leq g_M$ ($\forall x \in \mathbb{R}^n$) with $g_M \in \mathbb{R}$ the positive constant. Meanwhile, there exist non-negative functions $\zeta_M(x) \in \mathbb{R}$ and $d_M(x) \in \mathbb{R}$ such that, for all $x \in \mathbb{R}^n$

$$\left\|g^+(x)k(x)d(x)\right\| \leq \ell_M(x) \quad \text{and} \quad \|d(x)\| \leq d_M(x)$$

with $g^+(x)$ the Moore–Penrose pseudo-inverse of $g(x)$. In addition, $\ell_M(0) = 0$, $d(0) = 0$, and $d_M(0) = 0$.

This paper aims at finding an appropriate state feedback controller to stabilize system (1). Owing to the existence of system uncertainties, it is challengeable to design the stabilizing controller directly. To address this issue, we will convert the robust control problem of system (1) into a constrained optimal control problem of the auxiliary system.

B. Hamilton–Jacobi–Bellman Equation Related to Auxiliary Systems

Divide the term $k(x)d(x)$ into the following two parts:

$$k(x)d(x) = g(x)g^{+}(x)k(x)d(x) + h(x)d(x) \tag{2}$$

with

$$h(x) = \big(I_n - g(x)g^{+}(x)\big)k(x). \tag{3}$$

According to [40], the auxiliary system corresponding to (1) can be described as

$$\dot{x} = f(x) + g(x)u + h(x)\upsilon \tag{4}$$

where $u \in \mathfrak{U}$ and $\upsilon \in \mathbb{R}^p$ is the auxiliary control.

The infinite-horizon cost function for system (4) is given by

$$V^{u,\upsilon}(x(t)) = \int_t^{\infty} (\Psi(x(s)) + r(x(s), u(s), \upsilon(s)))\mathrm{d}s \tag{5}$$

where $\Psi(x) = 2\ell_M^2(x) + \rho d_M^2(x)$, $\rho \in \mathbb{R}$ is a positive constant, and

$$r(x, u, \upsilon) = x^{\mathsf{T}}Qx + \mathcal{W}(u) + \rho\upsilon^{\mathsf{T}}\upsilon$$

with $Q \in \mathbb{R}^{n\times n}$ the positive definite matrix and $\mathcal{W}(u) \in \mathbb{R}$ the semipositive definite function.

To overcome the bounded control, we define $\mathcal{W}(u)$ as [41]

$$\mathcal{W}(u) = 2\beta \sum_{i=1}^{m} \int_0^{u_i} \psi^{-1}(\zeta/\beta)\mathrm{d}\zeta \tag{6}$$

where $\psi(\cdot)$ is a bounded monotonic function with $\psi(0) = 0$. Meanwhile, $\psi(\cdot)$ is an odd function with its derivative bounded. Since $\psi^{-1}(\cdot)$ is a monotonic odd function, $\mathcal{W}(u)$ given in (6) is semipositive definite. In this paper, we let $\psi(\cdot)$ be the hyperbolic tangent function, i.e., $\psi(\cdot) = \tanh(\cdot)$.

Let $\mathscr{A}(\Omega)$ be the set of admissible control [5] defined on Ω. Then, the optimal value of (5) is formulated as

$$V^*(x) = \min_{u,\upsilon\in\mathscr{A}(\Omega)} V^{u,\upsilon}(x). \tag{7}$$

If $V^*(x)$ is continuously differentiable, then its derivative satisfies

$$\begin{aligned}&\big(V_x^*\big)^{\mathsf{T}}(f(x) + g(x)u + h(x)\upsilon)\\ &\quad + \Psi(x) + x^{\mathsf{T}}Qx + \mathcal{W}(u) + \rho\upsilon^{\mathsf{T}}\upsilon = 0.\end{aligned}$$

According to [4], the Hamiltonian for V_x^*, u, and υ can be defined as

$$\begin{aligned}H\big(x, V_x^*, u, \upsilon\big) = {}&\big(V_x^*\big)^{\mathsf{T}}(f(x) + g(x)u + h(x)\upsilon) + \Psi(x)\\ &+ x^{\mathsf{T}}Qx + \mathcal{W}(u) + \rho\upsilon^{\mathsf{T}}\upsilon.\end{aligned} \tag{8}$$

Then, $V^*(x)$ can be obtained by solving the Hamilton–Jacobi–Bellman (HJB) equation

$$\min_{u,\upsilon\in\mathscr{A}(\Omega)} H\big(x, V_x^*, u, \upsilon\big) = 0 \tag{9}$$

with $V^*(0) = 0$. Based on the stationary condition [42, Th. 5.8], we can therefore derive the closed-form expressions of optimal control and optimal auxiliary control as follows [4]:

$$u^*(x) = -\beta \tanh\bigg(\frac{1}{2\beta}g^{\mathsf{T}}(x)V_x^*\bigg) \tag{10}$$

$$\upsilon^*(x) = -\frac{1}{2\rho}h^{\mathsf{T}}(x)V_x^*. \tag{11}$$

From (8)–(11), we can rewrite the HJB equation as

$$\begin{aligned}&\big(V_x^*\big)^{\mathsf{T}}f(x) + \Psi(x) + x^{\mathsf{T}}Qx + \mathcal{W}\bigg(-\beta\tanh\bigg(\frac{1}{2\beta}g^{\mathsf{T}}(x)V_x^*\bigg)\bigg)\\ &\quad - \beta\big(V_x^*\big)^{\mathsf{T}}g(x)\tanh\bigg(\frac{1}{2\beta}g^{\mathsf{T}}(x)V_x^*\bigg) - \bigg\|\frac{1}{2\sqrt{\rho}}h^{\mathsf{T}}(x)V_x^*\bigg\|^2 = 0\end{aligned} \tag{12}$$

with $V^*(0) = 0$. According to [30], (12) is the time-triggered HJB equation.

Similar to [43], it can be proved that the robust controller for system (1) is able to be obtained by solving (12). However, owing to the use of time-triggered formulations, the robust control strategy is developed in the time-triggering mechanism. As mentioned in [44], the time-triggered control algorithms generally have low efficiency of using the limited communication resources between actuators and systems. In addition, they often involve high-computational burdens. To overcome the two deficiencies, we will develop a robust ETC scheme for system (1).

III. Robust ETC Strategy

In this section, we first describe the robust stabilization of system (1) in the ETM. Specifically, we prove that the robust ETC of (1) can be obtained by solving an ETHJB equation. Then, we use the SN-ACD to solve the ETHJB equation.

A. Robust Stabilization in the ETM

Let $\{t_j\}_{j=0}^{\infty}$ (*note:* $t_j < t_{j+1}, j \in \mathbb{N}$) be the sequence of triggering instants, where t_j denotes the jth triggering instant. The system state is sampled at the triggering instant t_j, and the sampled state is written as

$$\bar{x}_j = x\big(t_j\big) \quad j \in \mathbb{N}.$$

Since there generally exists an error between the sampled state $\bar{x}_j$ and the current state $x(t)$, we define the error as follows:

$$e_j(t) = \bar{x}_j - x(t) \quad \forall t \in \big[t_j, t_{j+1}\big). \tag{13}$$

From the expression $e_j(t)$ given in (13), we can judge whether an event is triggered or not. Specifically, if the event is triggered at instant $t = t_j$, then $e_j(t_j) = 0$. Based on the sampled state, we can obtain the ETC law $u(\bar{x}_j)$, which is executed at the triggering instant t_j. By using the zero-order hold technique [28], the control sequence $\{u(\bar{x}_j)\}_{j=0}^{\infty}$ can generate a continuous-time input signal $\mu(\bar{x}_j, t)$, i.e.,

$$\mu\big(\bar{x}_j, t\big) = u\big(\bar{x}_j\big) = u\big(x\big(t_j\big)\big) \quad \forall t \in \big[t_j, t_{j+1}\big).$$

Let the above mentioned ETM be applied to $u^*(x)$ given in (10). Then, the optimal ETC law for system (4) with the cost function (5) can be obtained as [30] (for all $t \in [t_j, t_{j+1})$)

$$\mu^*(\bar{x}_j, t) = u^*(\bar{x}_j) = -\beta \tanh\left(\frac{1}{2\beta} g^{\mathsf{T}}(\bar{x}_j) V^*_{\bar{x}_j}\right) \tag{14}$$

with $V^*_{\bar{x}_j} = (\partial V^*(x)/\partial x)|_{x=\bar{x}_j}$.

Similarly, applying the aforementioned ETM to $\upsilon^*(x)$ given in (11), we can derive the optimal auxiliary ETC law as

$$\vartheta^*(\bar{x}_j, t) = \upsilon^*(\bar{x}_j) = -\frac{1}{2\rho} h^{\mathsf{T}}(\bar{x}_j) V^*_{\bar{x}_j} \quad \forall t \in [t_j, t_{j+1}). \tag{15}$$

Remark 1: For brevity, in subsequent discussion we write $\mu^*(\bar{x}_j, t)$ and $\vartheta^*(\bar{x}_j, t)$ as $\mu^*(\bar{x}_j)$ and $\vartheta^*(\bar{x}_j)$, respectively.

Before continuing the discussion, we give the following assumption used in [30] and [45].

Assumption 3: $u^*(x)$ has the Lipschitz property on Ω. That is, there exists a Lipschitz constant $K_{u^*} > 0$ such that, for all $x, \bar{x}_j \in \Omega$

$$\left\| u^*(x) - u^*(\bar{x}_j) \right\| \le K_{u^*} \|x - \bar{x}_j\| = K_{u^*} \|e_j\|.$$

Remark 2: By using Remark 1 and (14), we can write $\mu^*(\bar{x}_j) = u^*(\bar{x}_j)$. Thus, Assumption 3 implies

$$\left\| u^*(x) - \mu^*(\bar{x}_j) \right\| \le K_{u^*} \|e_j\| \tag{16}$$

for all $x, \bar{x}_j \in \Omega$.

Theorem 1: Let Assumptions 1–3 be valid and let $V^*(x)$ be a solution of the HJB equation (12). Then, the optimal ETC law $\mu^*(\bar{x}_j)$ given in (14) can ensure the closed-loop system (1) to be stable in the sense of uniform ultimate boundedness only if $\upsilon^*(x)$ given in (11) satisfies

$$\left\| \upsilon^*(x(t)) \right\|^2 \le \lambda_{\min}(Q) \|x(t)\|^2 \quad \forall t \ge t_s \tag{17}$$

where $t_s \ge 0$ is a threshold, and provided that the triggering condition is given by

$$\|e_j\|^2 \le \frac{(1 - 2\rho)\lambda_{\min}(Q)}{4K^2_{u^*}} \|x\|^2 \triangleq \|e_T\|^2 \tag{18}$$

with $0 < \rho < 1/2$ the design parameter and e_T the triggering threshold.

Proof: We take $V^*(x)$ as the Lyapunov function candidate. From the expression $V^*(x)$ given as in (7), we can deduce that $V^*(x) > 0$ for $x \neq 0$ and $V^*(x) = 0 \Leftrightarrow x = 0$, i.e., $V^*(x)$ is positive definite.

By differentiating $V^*(x)$ along the solution of $\dot{x} = f(x) + g(x)\mu^*(\bar{x}_j) + k(x)d(x)$ and using (2), we have [*note:* $\dot{V}^*(x)$ denotes $\mathrm{d}V^*(x(t))/\mathrm{d}t$]

$$\begin{aligned}
\dot{V}^*(x) &= \left(V^*_x\right)^{\mathsf{T}}\left(f(x) + g(x)\mu^*(\bar{x}_j) + k(x)d(x)\right) \\
&= \left(V^*_x\right)^{\mathsf{T}}\left(f(x) + g(x)u^*(x) + h(x)\upsilon^*(x)\right) \\
&\quad + \left(V^*_x\right)^{\mathsf{T}} g(x)\left(\mu^*(\bar{x}_j) - u^*(x)\right) \\
&\quad + \left(V^*_x\right)^{\mathsf{T}} g(x) g^+(x) k(x) d(x) \\
&\quad + (V^*_x)^{\mathsf{T}} h(x)\left(d(x) - \upsilon^*(x)\right)
\end{aligned} \tag{19}$$

with $h(x)$ defined as in (3).

On the other hand, from (8) and (9), we obtain

$$\begin{aligned}
&\left(V^*_x\right)^{\mathsf{T}}\left(f(x) + g(x)u^*(x) + h(x)\upsilon^*(x)\right) \\
&\quad = -\Psi(x) - x^{\mathsf{T}}Qx - \mathcal{W}\left(u^*(x)\right) - \rho\left\|\upsilon^*(x)\right\|^2.
\end{aligned} \tag{20}$$

Meanwhile, from (10) and (11), we find

$$\begin{cases} \left(V^*_x\right)^{\mathsf{T}} g(x) = -2\beta\left(\tanh^{-1}(u^*(x)/\beta)\right)^{\mathsf{T}} \\ \left(V^*_x\right)^{\mathsf{T}} h(x) = -2\rho(\upsilon^*(x))^{\mathsf{T}}. \end{cases} \tag{21}$$

Substituting (20) and (21) into (19), it follows:

$$\begin{aligned}
\dot{V}^*(x) = &-\Psi(x) - x^{\mathsf{T}}Qx - \mathcal{W}\left(u^*(x)\right) + \rho\left\|\upsilon^*(x)\right\|^2 \\
&\underbrace{+2\beta\left(\tanh^{-1}\left(u^*(x)/\beta\right)\right)^{\mathsf{T}}\left(u^*(x) - \mu^*(\bar{x}_j)\right)}_{\pi_1} \\
&\underbrace{-2\beta\left(\tanh^{-1}\left(u^*(x)/\beta\right)\right)^{\mathsf{T}} g^+(x)k(x)d(x)}_{\pi_2} \\
&\underbrace{-2\rho\left(\upsilon^*(x)\right)^{\mathsf{T}} d(x)}_{\pi_3}.
\end{aligned} \tag{22}$$

By using Young's inequality $2y^{\mathsf{T}}z \le \varrho\|y\|^2 + \|z\|^2/\varrho$ ($\varrho > 0$) and (16), we can see that π_1 in (22) implies (*note:* $\varrho = 1/2$)

$$\begin{aligned}
\pi_1 &\le \frac{\beta^2}{2}\left\|\tanh^{-1}\left(u^*(x)/\beta\right)\right\|^2 + 2\left\|u^*(x) - \mu^*(\bar{x}_j)\right\|^2 \\
&\le \frac{\beta^2}{2}\sum_{i=1}^{m}\left(\tanh^{-1}(u^*_i(x)/\beta)\right)^2 + 2K^2_{u^*}\|e_j\|^2.
\end{aligned} \tag{23}$$

Similarly, by using the above mentioned Young's inequality and Assumption 2, we can find that π_2 and π_3 in (22) yield (*note:* $\varrho = 1/2$ and $\varrho = 1$, respectively)

$$\begin{aligned}
\pi_2 &\le \frac{\beta^2}{2}\left\|\tanh^{-1}\left(u^*(x)/\beta\right)\right\|^2 + 2\left\|g^+(x)k(x)d(x)\right\|^2 \\
&\le \frac{\beta^2}{2}\sum_{i=1}^{m}\left(\tanh^{-1}\left(u^*_i(x)/\beta\right)\right)^2 + 2\ell^2_M(x)
\end{aligned} \tag{24}$$

$$\pi_3 \le \rho\left\|\upsilon^*(x)\right\|^2 + \rho\|d(x)\|^2 \le \rho\left\|\upsilon^*(x)\right\|^2 + \rho d^2_M(x). \tag{25}$$

From [46] (*note:* see the proof of [46, Th. 1]), we know

$$\begin{aligned}
\mathcal{W}\left(u^*\right) &= 2\beta\sum_{i=1}^{m}\int_0^{u^*_i(x)} \tanh^{-1}(\zeta/\beta)\mathrm{d}\zeta \\
&= \beta^2\sum_{i=1}^{m}\left(\tanh^{-1}(u^*_i(x)/\beta)\right)^2 \\
&\quad - 2\beta^2\sum_{i=1}^{m}\int_0^{\tanh^{-1}\left(u^*_i(x)/\beta\right)} \tau_i \tanh^2(\tau_i)\mathrm{d}\tau_i.
\end{aligned} \tag{26}$$

Observing that $\Psi(x) = 2\ell^2_M(x) + \rho d^2_M(x)$ and using (23)–(26), we can conclude that (22) yields

$$\begin{aligned}
\dot{V}^*(x) \le &-x^{\mathsf{T}}Qx + 2\rho\left\|\upsilon^*(x)\right\|^2 + 2K^2_{u^*}\|e_j\|^2 \\
&\underbrace{+2\beta^2\sum_{i=1}^{m}\int_0^{\tanh^{-1}\left(u^*_i(x)/\beta\right)} \tau_i \tanh^2(\tau_i)\mathrm{d}\tau_i}_{\pounds(x)}.
\end{aligned} \tag{27}$$

According to the proof of [46, Th. 1], we know that $\pounds(x)$ given in (27) is a bounded function. To facilitate subsequent discussion, we denote that $\|\pounds(x)\| \le \epsilon_M$, where $\epsilon_M > 0$ is a constant. Then, (27) can be further rewritten as

$$\begin{aligned}\dot{V}^*(x) &\le -\lambda_{\min}(Q)\|x\|^2 + 2\rho\left\|\upsilon^*(x)\right\|^2 + 2K_{u^*}^2\|e_j\|^2 + \epsilon_M\\ &= -2\rho\left(\lambda_{\min}(Q)\|x\|^2 - \left\|\upsilon^*(x)\right\|^2\right) + 2K_{u^*}^2\|e_j\|^2\\ &\quad - (1-2\rho)\lambda_{\min}(Q)\|x\|^2 + \epsilon_M \end{aligned} \tag{28}$$

with $\lambda_{\min}(Q)$ the minimum eigenvalue of Q.

Thus, if (17) and (18) hold, then (28) yields

$$\dot{V}^*(x) \le -\frac{(1-2\rho)\lambda_{\min}(Q)}{2}\|x\|^2 + \epsilon_M. \tag{29}$$

Therefore, from (29), we can find that $\dot{V}^*(x) < 0$ only when $x(t)$ is out of the following set:

$$\Omega_x = \left\{x\colon \|x\| \le \sqrt{\frac{2\epsilon_M}{(1-2\rho)\lambda_{\min}(Q)}}\right\}.$$

Then, uniform ultimate boundedness of the states of system (1) is guaranteed by using Lyapunov extension theorem [47]. Specifically, this indicates that $\mu^*(\bar{x}_j)$ keeps the closed-loop system (1) stable in the sense of uniform ultimate boundedness. Meanwhile, the ultimate bound is $\sqrt{2\epsilon_M/((1-2\rho)\lambda_{\min}(Q))}$. ■

Remark 3: According to (18), the triggering instant t_j can be calculated. Then, it is possible to obtain the minimal intersample time $(\Delta t_j)_{\min}$, where $\Delta t_j = t_{j+1} - t_j$, $j \in \mathbb{N}$. However, if there exists $(\Delta t_j)_{\min} = 0$, then the Zeno behavior occurs [48]. In this circumstance, $\mu^*(\bar{x}_j)$ has to be redesigned. Fortunately, $(\Delta t_j)_{\min} > 0$, $j \in \mathbb{N}$, under Assumption 1 (*note:* since similar proofs have been provided in [36] and [49], we omit the proof here). In this paper, simulation results provided in Section V also show that $(\Delta t_j)_{\min} > 0$, $j \in \mathbb{N}$.

To obtain the optimal ETC law $\mu^*(\bar{x}_j)$, we need to solve the ETHJB equation, which is derived by substituting (14) and (15) into (9). That is,

$$\begin{aligned}&\left(V_x^*\right)^{\mathsf T} f(x) - \beta\left(V_x^*\right)^{\mathsf T} g(x)\tanh\left(\frac{1}{2\beta}g^{\mathsf T}(\bar{x}_j)V_{\bar{x}_j}^*\right)\\ &\quad - \frac{1}{2\rho}(V_x^*)^{\mathsf T} h(x)h^{\mathsf T}(\bar{x}_j)V_{\bar{x}_j}^* + \Psi(x) + x^{\mathsf T}Qx\\ &\quad + \mathcal{W}\left(-\beta\tanh\left(\frac{1}{2\beta}g^{\mathsf T}(\bar{x}_j)V_{\bar{x}_j}^*\right)\right) + \left\|\frac{1}{2\sqrt{\rho}}h^{\mathsf T}(\bar{x}_j)V_{\bar{x}_j}^*\right\|^2 = 0. \end{aligned} \tag{30}$$

Generally, it is rather hard to solve the ETHJB equation (30) analytically [50]. To conquer the difficulty, we present the SN-ACD to approximately solve (30).

B. SN-ACD for Solving the ETHJB Equation

The approximation theorem [51] guarantees that $V^*(x)$ given in (7) can be represented via a critic network over Ω as

$$V^*(x) = \omega_c^{\mathsf T}\sigma_c(x) + \varepsilon_c(x)$$

where $\omega_c \in \mathbb{R}^{\tilde{n}_c}$ is the ideal weight vector, $\sigma_c(x) = [\sigma_{c1}(x), \sigma_{c2}(x), \ldots, \sigma_{c\tilde{n}_c}(x)]^{\mathsf T} \in \mathbb{R}^{\tilde{n}_c}$ is the basis function vector, $\sigma_{c\iota}(x)$, $\iota = 1, 2, \ldots, \tilde{n}_c$, are continuously differentiable functions with $\sigma_{c\iota}(0) = 0$, $\tilde{n}_c \in \mathbb{N}^+$ is the number of basis functions, and $\varepsilon_c(x) \in \mathbb{R}$ is the approximation error.

Differentiating $V^*(x)$ at the sampled state $\bar{x}_j$, we have

$$V_{\bar{x}_j}^* = \nabla\sigma_c^{\mathsf T}(\bar{x}_j)\omega_c + \nabla\varepsilon_c(\bar{x}_j) \quad \forall t \in [t_j, t_{j+1}) \tag{31}$$

where $\nabla\sigma_c(\bar{x}_j) = (\partial\sigma_c(x)/\partial x)|_{x=\bar{x}_j}$ and $\nabla\varepsilon_c(\bar{x}_j) = (\partial\varepsilon_c(x)/\partial x)|_{x=\bar{x}_j}$.

Substituting (31) into (14), we can rewrite $\mu^*(\bar{x}_j)$ as

$$\mu^*(\bar{x}_j) = -\beta\tanh(\mathcal{A}_1(\bar{x}_j)) + \varepsilon_{\mu^*}(\bar{x}_j) \quad \forall t \in [t_j, t_{j+1}) \tag{32}$$

where

$$\mathcal{A}_1(\bar{x}_j) = \frac{1}{2\beta}g^{\mathsf T}(\bar{x}_j)\nabla\sigma_c^{\mathsf T}(\bar{x}_j)\omega_c$$

and $\varepsilon_{\mu^*}(\bar{x}_j) = -(1/2)(\underline{\mathbf{1}} - \tanh^2(\xi))g^{\mathsf T}(\bar{x}_j)\nabla\varepsilon_c(\bar{x}_j)$ with $\underline{\mathbf{1}} = [1, \ldots, 1]^{\mathsf T} \in \mathbb{R}^m$ and ξ chosen between $\mathcal{A}_0(\bar{x}_j)$ (*note:* $\mathcal{A}_0(\bar{x}_j) = (1/(2\beta))g^{\mathsf T}(\bar{x}_j)V_{\bar{x}_j}^*$) and $\mathcal{A}_1(\bar{x}_j)$.

Similarly, by using (31), $\vartheta^*(\bar{x}_j)$ given in (15) can be represented as (for all $t \in [t_j, t_{j+1})$)

$$\vartheta^*(\bar{x}_j) = -\frac{1}{2\rho}h^{\mathsf T}(\bar{x}_j)\nabla\sigma_c^{\mathsf T}(\bar{x}_j)\omega_c + \varepsilon_{\vartheta^*}(\bar{x}_j) \tag{33}$$

with $\varepsilon_{\vartheta^*}(\bar{x}_j) = -(1/2\rho)h^{\mathsf T}(\bar{x}_j)\nabla\varepsilon_c(\bar{x}_j)$.

Remark 4: The difference between $\varepsilon_{\mu^*}(\bar{x}_j)$ given in (32) and $\varepsilon_{\vartheta^*}(\bar{x}_j)$ given in (33) is caused by control constraints (*note:* u is constrained while υ is unconstrained). To make (32) be better for understanding, we provide the detailed process of deriving $\varepsilon_{\mu^*}(\bar{x}_j)$ as follows. Let

$$\mathcal{T}(\mathcal{A}_\varpi(x)) = -\beta\tanh(\mathcal{A}_\varpi(x)), \quad \varpi = 0, 1.$$

Then, applying the mean value theorem [42, Th. 5.10] to $\mathcal{T}(\mathcal{A}_\varpi(x))$, we obtain (*note:* $\mathcal{A}_0(x) = (1/(2\beta))g^{\mathsf T}(x)V_x^*$)

$$\begin{aligned}\mathcal{T}(\mathcal{A}_0(x)) - \mathcal{T}(\mathcal{A}_1(x)) &= -\beta(\tanh(\mathcal{A}_0(x)) - \tanh(\mathcal{A}_1(x)))\\ &= -\frac{1}{2}\left(\underline{\mathbf{1}} - \tanh^2(\xi)\right)g^{\mathsf T}(x)\nabla\varepsilon_c(x)\end{aligned}$$

with ξ chosen between $\mathcal{A}_0(x)$ and $\mathcal{A}_1(x)$. By using (31), we find that (14) yields

$$\begin{aligned}\mu^*(\bar{x}_j) &= -\beta\tanh(\mathcal{A}_0(\bar{x}_j))\\ &= \mathcal{T}(\mathcal{A}_1(\bar{x}_j)) + \left(\mathcal{T}(\mathcal{A}_0(\bar{x}_j)) - \mathcal{T}(\mathcal{A}_1(\bar{x}_j))\right)\\ &= -\beta\tanh(\mathcal{A}_1(\bar{x}_j)) - \frac{1}{2}\left(\underline{\mathbf{1}} - \tanh^2(\xi)\right)g^{\mathsf T}\nabla\varepsilon_c(\bar{x}_j).\end{aligned}$$

Hence, we can obtain the expression $\varepsilon_{\mu^*}(\bar{x}_j)$ given as in (32).

In general, the ideal weight vector ω_c is unavailable. Thus, we cannot implement $\mu^*(\bar{x}_j)$ given in (32). To handle this issue, we replace ω_c with the current estimated weight vector $\hat{\omega}_c$ in the critic network. Then, the approximation value function can be formulated as

$$\hat{V}(x) = \hat{\omega}_c^{\mathsf T}\sigma_c(x). \tag{34}$$

The derivative of $\hat{V}(x)$ at the sampled state $\bar{x}_j$ is

$$\hat{V}_{\bar{x}_j} = \nabla\sigma_c^{\mathsf T}(\bar{x}_j)\hat{\omega}_c.$$

Replacing $V_{\bar{x}_j}^*$ in (14) with $\hat{V}_{\bar{x}_j}$, we derive the estimated value of $\mu^*(\bar{x}_j)$ as

$$\hat{\mu}(\bar{x}_j) = -\beta\tanh(\mathcal{A}_2(\bar{x}_j)) \quad \forall t \in [t_j, t_{j+1}) \tag{35}$$

where

$$\mathcal{A}_2(\bar{x}_j) = \frac{1}{2\beta} g^{\mathsf{T}}(\bar{x}_j)\nabla\sigma_c^{\mathsf{T}}(\bar{x}_j)\hat{\omega}_c.$$

By the same token, the estimated value of $\vartheta^*(\bar{x}_j)$ given in (33) can be obtained as

$$\hat{\vartheta}(\bar{x}_j) = -\frac{1}{2\rho} h^{\mathsf{T}}(\bar{x}_j)\nabla\sigma_c^{\mathsf{T}}(\bar{x}_j)\hat{\omega}_c \quad \forall t \in [t_j, t_{j+1}). \tag{36}$$

Substituting $\hat{V}(x)$, $\hat{\mu}(\bar{x}_j)$, and $\hat{\vartheta}(\bar{x}_j)$ into (8), we can see that the approximation Hamiltonian is

$$\begin{aligned}
&\hat{H}\Big(x, \hat{V}_x, \hat{\mu}(\bar{x}_j), \hat{\vartheta}(\bar{x}_j)\Big)\\
&= \hat{\omega}_c^{\mathsf{T}}\nabla\sigma_c(x)\Big(f(x) + g(x)\hat{\mu}(\bar{x}_j) + h(x)\hat{\vartheta}(\bar{x}_j)\Big)\\
&\quad + \Psi(x) + x^{\mathsf{T}}Qx + \mathcal{W}\Big(\hat{\mu}^{\mathsf{T}}(\bar{x}_j)\Big) + \rho\Big\|\hat{\vartheta}(\bar{x}_j)\Big\|^2.
\end{aligned}$$

Observe that (9) implies

$$H\big(x, V_x^*, \mu^*(\bar{x}_j), \vartheta^*(\bar{x}_j)\big) = 0.$$

Thus, the error of Hamiltonian can be formulated as

$$\begin{aligned}
e_c &= \hat{H}\Big(x, \hat{V}_x, \hat{\mu}(\bar{x}_j), \hat{\vartheta}(\bar{x}_j)\Big) - H\big(x, V_x^*, \mu^*(\bar{x}_j), \vartheta^*(\bar{x}_j)\big)\\
&= \hat{\omega}_c^{\mathsf{T}}\phi + \Psi(x) + x^{\mathsf{T}}Qx + \mathcal{W}\big(\hat{\mu}(\bar{x}_j)\big) + \rho\Big\|\hat{\vartheta}(\bar{x}_j)\Big\|^2
\end{aligned} \tag{37}$$

where $\phi = \nabla\sigma_c(x)(f(x) + g(x)\hat{\mu}(\bar{x}_j) + h(x)\hat{\vartheta}(\bar{x}_j))$.

To ensure e_c given in (37) to be sufficiently small, we use the gradient descent method to minimize the target function $E = (1/2)e_c^{\mathsf{T}}e_c$. Then, the weight update rule for the critic network is obtained as

$$\begin{aligned}
\dot{\hat{\omega}}_c &= -\frac{l_c}{\left(1 + \phi^{\mathsf{T}}\phi\right)^2}\frac{\partial E}{\partial\hat{\omega}_c}\\
&= -\frac{l_c\phi}{\left(1 + \phi^{\mathsf{T}}\phi\right)^2}e_c \quad \forall t \in \big[t_j, t_{j+1}\big)
\end{aligned} \tag{38}$$

with e_c defined as in (37), $l_c \in \mathbb{R}^n$ the positive parameter, and $(1 + \phi^{\mathsf{T}}\phi)^{-2}$ the normalization term.

Let the weight estimation error of the critic network be $\tilde{\omega}_c = \omega_c - \hat{\omega}_c$. Then, from (38), we can see that the weight estimation error dynamics of the critic network satisfies [30]

$$\dot{\tilde{\omega}}_c = -l_c\varphi\varphi^{\mathsf{T}}\tilde{\omega}_c + \frac{l_c\varphi}{1 + \phi^{\mathsf{T}}\phi}\varepsilon_H \quad \forall t \in [t_j, t_{j+1}) \tag{39}$$

where $\varphi = \phi/(1 + \phi^{\mathsf{T}}\phi)^2$ and $\varepsilon_H = -\nabla\varepsilon_c^{\mathsf{T}}(x)(f(x) + g(x)\hat{\mu}(\bar{x}_j) + h(x)\hat{\vartheta}(\bar{x}_j))$ is the residual error.

From the ETM introduced in Section III-A, we can find that the closed-loop system (4) is a hybrid system. Let the augmented state be $\mathcal{X} = [x^{\mathsf{T}}, \bar{x}_j^{\mathsf{T}}, \tilde{\omega}_c^{\mathsf{T}}]^{\mathsf{T}}$. Then, we can describe the hybrid dynamical system as follows.

1) *Continuous Dynamics:*

$$\dot{\mathcal{X}}(t) = \begin{bmatrix} f(x) + \mathcal{F}\big(x, \bar{x}_j\big) \\ 0 \\ -l_c\varphi\varphi^{\mathsf{T}}\tilde{\omega}_c + \dfrac{l_c\varphi\varepsilon_H}{\left(1 + \phi^{\mathsf{T}}\phi\right)^2} \end{bmatrix} \forall t \in [t_j, t_{j+1}) \tag{40}$$

where

$$\begin{aligned}
\mathcal{F}\big(x, \bar{x}_j\big) = &-\beta g(x)\tanh\left(\frac{1}{2\beta}g^{\mathsf{T}}(\bar{x}_j)\nabla\sigma_c^{\mathsf{T}}(\bar{x}_j)\hat{\omega}_c\right)\\
&- \frac{1}{2\rho}h(x)h^{\mathsf{T}}(\bar{x}_j)\nabla\sigma_c^{\mathsf{T}}(\bar{x}_j)\hat{\omega}_c.
\end{aligned}$$

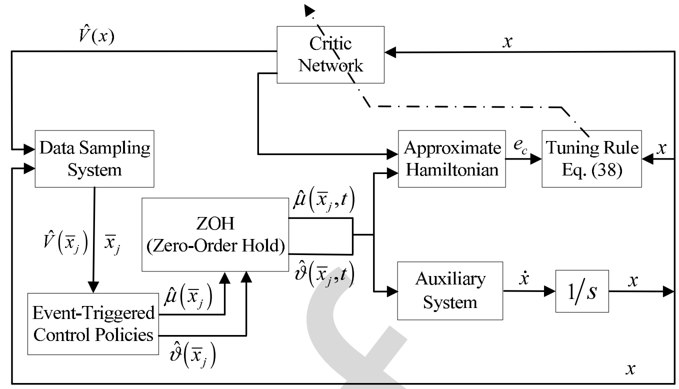

Fig. 1. Block diagram of the proposed ETC strategy.

2) *Discrete Dynamics:*

$$\mathcal{X}\big(t^+\big) = \mathcal{X}(t) + \begin{bmatrix} 0 \\ \bar{x}_j - x(t) \\ 0 \end{bmatrix} \quad t = t_{j+1} \tag{41}$$

where $\mathcal{X}(t^+) = \lim_{\eta\to 0^+}\mathcal{X}(t+\eta)$ with $\eta \in (0, t_{j+1} - t_j)$.

Based on the above mentioned analyses, we present the block diagram of the proposed ETC strategy in Fig. 1.

IV. Stability Analysis

Before proving stabilities of systems (40) and (41), we provide two assumptions introduced in [4] and [52], respectively.

Assumption 4: The derivative of the basic function vector is bounded as $\|\nabla\sigma_c(x)\| \le b_{\sigma_c}$ ($\forall x \in \Omega$), where b_{σ_c} is a positive constant. In addition, there exist positive constants $b_{\varepsilon_{\mu^*}}$, $b_{\varepsilon_{\vartheta^*}}$, and b_{ε_H} such the approximation errors $\varepsilon_{\mu^*}(\bar{x}_j)$, $\varepsilon_{\vartheta^*}(\bar{x}_j)$, and the residual error ε_H bounded as $\|\varepsilon_{\mu^*}(\bar{x}_j)\| \le b_{\varepsilon_{\mu^*}}$, $\|\varepsilon_{\vartheta^*}(\bar{x}_j)\| \le b_{\varepsilon_{\vartheta^*}}$, and $\|\varepsilon_H\| \le b_{\varepsilon_H}$ ($\forall\bar{x}_j, x \in \Omega$), respectively.

Similar to (16) imposed on $u^*(x)$, we present the following assumption for $\upsilon^*(x)$.

Assumption 5: $\upsilon^*(x)$ satisfies the Lipschitz condition on Ω. That is, for all $x, \bar{x}_j \in \Omega$, there exists a Lipschitz constant $K_{\upsilon^*} > 0$ such that

$$\big\|\upsilon^*(x) - \vartheta^*(\bar{x}_j)\big\| \le K_{\upsilon^*}\|x - \bar{x}_j\| = K_{\upsilon^*}\|e_j\|.$$

Let

$$G(\mathcal{A}_\kappa(x)) = \beta\tanh(\mathcal{A}_\kappa(x)), \ \kappa = 1, 2 \tag{42}$$

where $\mathcal{A}_1(x) = (1/(2\beta))g^{\mathsf{T}}(x)\nabla\sigma_c^{\mathsf{T}}(x)\omega_c$ and $\mathcal{A}_2(x) = (1/(2\beta))g^{\mathsf{T}}(x)\nabla\sigma_c^{\mathsf{T}}(x)\hat{\omega}_c$. Then, using Taylor's theorem [42], it follows:

$$\begin{aligned}
G(\mathcal{A}_1(x)) = &\ G(\mathcal{A}_2(x)) + \frac{\partial G(\mathcal{A}_2)}{\partial\mathcal{A}_2}(\mathcal{A}_1(x) - \mathcal{A}_2(x))\\
&+ O\Big((\mathcal{A}_1(x) - \mathcal{A}_2(x))^2\Big)\\
= &\ G(\mathcal{A}_2(x)) + \frac{1}{2}(I_m - \mathscr{B}(\mathcal{A}_2(x)))g^{\mathsf{T}}(x)\\
&\times \nabla\sigma_c^{\mathsf{T}}(x)\tilde{\omega}_c + O\Big((\mathcal{A}_1(x) - \mathcal{A}_2(x))^2\Big)
\end{aligned} \tag{43}$$

with $\mathscr{B}(\mathcal{A}_2(x)) = \mathrm{diag}\{\tanh^2(\mathcal{A}_{2i}(x))\}$, $i = 1, 2, \ldots, m$, and the high-order term $O((\mathcal{A}_1(x) - \mathcal{A}_2(x))^2)$.

Lemma 1: The high-order term given in (43) is bounded as

$$\left\| O\Big((\mathcal{A}_1(x) - \mathcal{A}_2(x))^2 \Big) \right\| \le 2\sqrt{m} + g_M b_{\sigma_c} \|\tilde{\omega}_c\|. \tag{44}$$

Proof: From (43), we can find

$$\begin{aligned} \left\| O\Big((\mathcal{A}_1(x) - \mathcal{A}_2(x))^2 \Big) \right\| &\le \|G(\mathcal{A}_1(x))\| + \|G(\mathcal{A}_2(x))\| \\ &\quad + \frac{1}{2} \|I_m - \mathscr{B}(\mathcal{A}_2(x))\| \|g(x)\| \\ &\quad \times \|\nabla\sigma(x)\| \|\tilde{\omega}_c\|. \end{aligned} \tag{45}$$

Since $\|\tanh(x)\| \le 1$ for all $x \in \mathbb{R}^n$, we can conclude that $\|G(\mathcal{A}_\kappa(x))\| = (\sum_{i=1}^{m} \tanh^2(\mathcal{A}_{\kappa i}(x)))^{1/2} \le \sqrt{m}$, $\kappa = 1, 2$, and $\|I_m - \mathscr{B}(\mathcal{A}_2(x))\| \le 2$. Then, using Assumptions 2 and 4, we can see that (45) yields (44). ■

Theorem 2: Consider auxiliary system (4) associated with the ETHJB equation (30). Let Assumptions 1–5 be valid and take the control policies proposed as in (35) and (36). Suppose that the initial control for system (4) is admissible and the weight tuning rule for the critic network is described as (38). Then, the closed-loop system (4) and the weight estimation error $\tilde{\omega}_c$ are UUB only if the following event-triggering condition holds:

$$\|e_j\|^2 \le \frac{(1-2\gamma)\lambda_{\min}(Q)}{4K_{\max}^2} \|x\|^2 \triangleq \|\bar{e}_T\|^2 \tag{46}$$

where $K_{\max} = \max\{K_{u^*}, K_{\upsilon^*}\}$, $0 < \gamma < 1/2$ is a design parameter, and $\bar{e}_T$ is the triggering threshold, and provided that the following inequality holds:

$$\frac{l_c}{2} \lambda_{\min}\Big(\varphi\varphi^{\mathsf{T}}\Big) - \Big(16 g_M^2 + h_M^2/\rho^2\Big) b_{\sigma_c}^2 > 0 \tag{47}$$

where $\lambda_{\min}(\varphi\varphi^{\mathsf{T}})$ denotes the minimum eigenvalue of $\varphi\varphi^{\mathsf{T}}$, φ satisfies the PE condition, and h_M is the bound of $h(x)$.

Proof: We take the Lyapunov function candidate as

$$L(t) = \underbrace{V^*(\bar{x}_j)}_{L_1(t)} + \underbrace{V^*(x(t))}_{L_2(t)} + \underbrace{(1/2)\tilde{\omega}_c^{\mathsf{T}}\tilde{\omega}_c}_{L_3(t)}.$$

Since the closed-loop system (4) is a hybrid system, we present the stability analysis from following two circumstances.

Situation I: Events are not triggered, i.e., $t \in [t_j, t_{j+1})$, $j \in \mathbb{N}$. Then, we have $\dot{L}_1(t) = \dot{V}^*(\bar{x}_j) = 0$.

Taking the derivative of $L_2(t)$ and using the trajectory generated from $\dot{x} = f(x) + g(x)\hat{\mu}(\bar{x}_j) + h(x)\hat{\vartheta}(\bar{x}_j)$, we have

$$\begin{aligned} \dot{L}_2(t) &= \big(V_x^*\big)^{\mathsf{T}} \Big(f(x) + g(x)\hat{\mu}(\bar{x}_j) + h(x)\hat{\vartheta}(\bar{x}_j) \Big) \\ &= \big(V_x^*\big)^{\mathsf{T}} \big(f(x) + g(x)u^*(x) + h(x)\upsilon^*(x) \big) \\ &\quad + \big(V_x^*\big)^{\mathsf{T}} g(x) \big(\hat{\mu}(\bar{x}_j) - u^*(x)\big) \\ &\quad + \big(V_x^*\big)^{\mathsf{T}} h(x) \Big(\hat{\vartheta}(\bar{x}_j) - \upsilon^*(x)\Big). \end{aligned} \tag{48}$$

Substituting (20) and (21) into (48), it follows:

$$\begin{aligned} \dot{L}_2(t) &= -\Psi(x) - x^{\mathsf{T}}Qx - \rho\big\|\upsilon^*(x)\big\|^2 - \mathcal{W}\big(u^*(x)\big) \\ &\quad \underbrace{+\, 2\beta\Big(\tanh^{-1}\big(u^*(x)/\beta\big)\Big)^{\mathsf{T}}\big(u^*(x) - \hat{\mu}(\bar{x}_j)\big)}_{\Xi} \\ &\quad + 2\rho\big(\upsilon^*(x)\big)^{\mathsf{T}}\Big(\upsilon^*(x) - \hat{\vartheta}(\bar{x}_j)\Big). \end{aligned} \tag{49}$$

Applying Young's inequality $2y^{\mathsf{T}}z \le \|y\|^2 + \|z\|^2$ to Ξ in (49), we obtain

$$\begin{aligned} \Xi &\le \beta^2 \Big\| \tanh^{-1}\big(u^*(x)/\beta\big) \Big\|^2 + \big\|u^*(x) - \hat{\mu}(\bar{x}_j)\big\|^2 \\ &= \beta^2 \sum_{i=1}^{m} \Big(\tanh^{-1}(u_i^*(x)/\beta) \Big)^2 + \big\|u^*(x) - \hat{\mu}(\bar{x}_j)\big\|^2. \end{aligned}$$

Then, by using (26), we can see that

$$-\mathcal{W}\big(u^*(x)\big) + \Xi \le \pounds(x) + \big\|u^*(x) - \hat{\mu}(\bar{x}_j)\big\|^2 \tag{50}$$

with $\pounds(x)$ defined as in (27). As indicated in the proof of Theorem 1, $\pounds(x)$ is bounded as $\|\pounds(x)\| \le \epsilon_M$. Thus, combining (49) and (50), we have

$$\begin{aligned} \dot{L}_2(t) &\le -\Psi(x) - x^{\mathsf{T}}Qx - \rho\Big\|\hat{\vartheta}(\bar{x}_j)\Big\|^2 + \epsilon_M \\ &\quad + \underbrace{\big\|u^*(x) - \hat{\mu}(\bar{x}_j)\big\|^2}_{\Lambda_1} + \underbrace{\rho\Big\|\upsilon^*(x) - \hat{\vartheta}(\bar{x}_j)\Big\|^2}_{\Lambda_2}. \end{aligned} \tag{51}$$

Applying the inequality $\|y+z\|^2 \le 2\|y\|^2 + 2\|z\|^2$ to Λ_1 in (51) and using Assumption 3 as well as (32) and (35), it follows:

$$\begin{aligned} \Lambda_1 &= \big\| \big(u^*(x) - \mu^*(\bar{x}_j)\big) + \big(\mu^*(\bar{x}_j) - \hat{\mu}(\bar{x}_j)\big) \big\|^2 \\ &\le 2\big\|\mu^*(\bar{x}_j) - \hat{\mu}(\bar{x}_j)\big\|^2 + 2\big\|u^*(x) - \mu^*(\bar{x}_j)\big\|^2 \\ &\le 2\big\|G\big(\mathcal{A}_2(\bar{x}_j)\big) - G\big(\mathcal{A}_1(\bar{x}_j)\big) + \varepsilon_{\mu^*}(\bar{x}_j)\big\|^2 + 2K_{u^*}^2\|e_j\|^2 \end{aligned} \tag{52}$$

where $G(\mathcal{A}_\kappa(\bar{x}_j)) = G(\mathcal{A}_\kappa(x))|_{x=\bar{x}_j}$ with $G(\mathcal{A}_\kappa(x))$ defined as in (42). By using (43) and Lemma 1 as well as Young's inequality, we derive

$$\begin{aligned} &2\big\|G\big(\mathcal{A}_2(\bar{x}_j)\big) - G\big(\mathcal{A}_1(\bar{x}_j)\big) + \varepsilon_{\mu^*}(\bar{x}_j)\big\|^2 \\ &\quad \le 2\Big(2g_M b_{\sigma_c}\|\tilde{\omega}_c\| + 2\sqrt{m} + b_{\varepsilon_{\mu^*}}\Big)^2 \\ &\quad \le 16 g_M^2 b_{\sigma_c}^2 \|\tilde{\omega}_c\|^2 + 4a_0^2 \end{aligned} \tag{53}$$

with $a_0 = 2\sqrt{m} + b_{\varepsilon_{\mu^*}}$.

Thus, combining (52) and (53), it follows:

$$\Lambda_1 \le 2K_{u^*}^2\|e_j\|^2 + 16 g_M^2 b_{\sigma_c}^2 \|\tilde{\omega}_c\|^2 + 4a_0^2. \tag{54}$$

Similar to the process of calculating Λ_1, we obtain

$$\begin{aligned} \Lambda_2 &= \Big\| \big(\upsilon^*(x) - \vartheta^*(\bar{x}_j)\big) + \Big(\vartheta^*(\bar{x}_j) - \hat{\vartheta}(\bar{x}_j)\Big) \Big\|^2 \\ &\le 2\Big\|\vartheta^*(\bar{x}_j) - \hat{\vartheta}(\bar{x}_j)\Big\|^2 + 2\big\|\upsilon^*(x) - \vartheta^*(\bar{x}_j)\big\|^2 \\ &\le 2\left\| -\frac{h^{\mathsf{T}}(\bar{x}_j)}{2\rho} \nabla\sigma_c^{\mathsf{T}}(\bar{x}_j)\tilde{\omega}_c + \varepsilon_{\vartheta^*}(\bar{x}_j) \right\|^2 + 2K_{\upsilon^*}^2\|e_j\|^2 \\ &\le 2K_{\upsilon^*}^2\|e_j\|^2 + \Big(h_M^2 b_{\sigma_c}^2/\rho^2\Big)\|\tilde{\omega}_c\|^2 + 4b_{\varepsilon_{\vartheta^*}}^2. \end{aligned} \tag{55}$$

Note that $\Psi(x)$ given in (5) and $\rho\|\hat{\vartheta}(\bar{x}_j)\|^2$ are non-negative functions. Then, from (51), (54), and (55), we get

$$\begin{aligned} \dot{L}_2(t) &\le -\lambda_{\min}(Q)\|x\|^2 + 4K_{\max}^2\|e_j\|^2 \\ &\quad + \Big(16 g_M^2 + h_M^2/\rho^2\Big) b_{\sigma_c}^2 \|\tilde{\omega}_c\|^2 + 4a_0^2 + 4b_{\varepsilon_{\vartheta^*}}^2 + \epsilon_M \end{aligned} \tag{56}$$

with $K_{\max} = \max\{K_{u^*}, K_{\upsilon^*}\}$.

Taking the time derivative of $L_3(t)$ and using the weight estimation error dynamics (39), it follows:

$$\dot{L}_3(t) = -l_c \tilde{\omega}_c^{\mathsf{T}} \varphi \varphi^{\mathsf{T}} \tilde{\omega}_c + l_c \frac{\tilde{\omega}_c^{\mathsf{T}} \varphi}{1 + \phi^{\mathsf{T}} \phi} \varepsilon_H. \tag{57}$$

Noticing that $1 + \phi^{\mathsf{T}}\phi \geq 1$ and using the above mentioned Young's inequality, we develop the last term in (57) as

$$\begin{aligned} \frac{l_c}{1 + \phi^{\mathsf{T}}\phi} \tilde{\omega}_c^{\mathsf{T}} \varphi \varepsilon_H &\leq \frac{l_c}{2\left(1 + \phi^{\mathsf{T}}\phi\right)} \left(\tilde{\omega}_c^{\mathsf{T}} \varphi \varphi^{\mathsf{T}} \tilde{\omega}_c + \varepsilon_H^{\mathsf{T}} \varepsilon_H \right) \\ &\leq \frac{l_c}{2} \tilde{\omega}_c^{\mathsf{T}} \varphi \varphi^{\mathsf{T}} \tilde{\omega}_c + \frac{l_c}{2} \varepsilon_H^{\mathsf{T}} \varepsilon_H. \end{aligned}$$

Then, (57) yields

$$\begin{aligned} \dot{L}_3(t) &\leq -\frac{l_c}{2} \tilde{\omega}_c^{\mathsf{T}} \varphi \varphi^{\mathsf{T}} \tilde{\omega}_c + \frac{l_c}{2} \varepsilon_H^{\mathsf{T}} \varepsilon_H \\ &\leq -\frac{l_c}{2} \lambda_{\min}\left(\varphi \varphi^{\mathsf{T}}\right) \|\tilde{\omega}_c\|^2 + \frac{l_c}{2} b_{\varepsilon_H}^2. \end{aligned} \tag{58}$$

By using (56) and (58), we can see that

$$\begin{aligned} \dot{L}(t) \leq\ & -2\gamma \lambda_{\min}(Q) \|x\|^2 - (1 - 2\gamma) \lambda_{\min}(Q) \|x\|^2 \\ & - \left(\frac{l_c}{2} \lambda_{\min}\left(\varphi \varphi^{\mathsf{T}}\right) - \left(16 g_M^2 + h_M^2/\rho^2\right) b_{\sigma_c}^2 \right) \|\tilde{\omega}_c\|^2 \\ & + 4K_{\max}^2 \|e_j\|^2 + 4a_0^2 + 4b_{\varepsilon_{\vartheta^*}}^2 + \epsilon_M. \end{aligned} \tag{59}$$

If the condition (46) holds, then (59) yields

$$\begin{aligned} \dot{L}(t) \leq\ & -2\gamma \lambda_{\min}(Q) \|x\|^2 + 4a_0^2 + 4b_{\varepsilon_{\vartheta^*}}^2 + \epsilon_M \\ & - \left(\frac{l_c}{2} \lambda_{\min}\left(\varphi \varphi^{\mathsf{T}}\right) - \left(16 g_M^2 + h_M^2/\rho^2\right) b_{\sigma_c}^2 \right) \|\tilde{\omega}_c\|^2. \end{aligned}$$

Under the condition (47), we can find that $\dot{L}(t) < 0$ only if we can ensure one of the following inequalities holds:

$$\|x\| > \sqrt{\frac{4a_0^2 + 4b_{\varepsilon_{\vartheta^*}}^2 + \epsilon_M}{2\gamma \lambda_{\min}(Q)}} \triangleq c_1 \tag{60}$$

or

$$\|\tilde{\omega}_c\| > \sqrt{\frac{8a_0^2 + 8b_{\varepsilon_{\vartheta^*}}^2 + 2\epsilon_M}{l_c \lambda_{\min}\left(\varphi \varphi^{\mathsf{T}}\right) - \left(32 g_M^2 + 2h_M^2/\rho^2\right) b_{\sigma_c}^2}} \triangleq c_2. \tag{61}$$

Then, uniform ultimate boundedness of both $x(t)$ and $\tilde{\omega}_c$ is obtained by using Lyapunov extension theorem [47]. Meanwhile, the ultimate bounds of $x(t)$ and $\tilde{\omega}_c$ are c_1 given in (60) and c_2 given in (61), respectively.

Situation II: Events are triggered, i.e., $t = t_j, j \in \mathbb{N}$. Then, we take the difference of Lyapunov function candidate $L(t_j)$ into account, that is

$$\Delta L(t_j) = V^*(\bar{x}_{j+1}) - V^*(\bar{x}_j) + \Pi\left(x\left(t_j^+\right), \bar{x}_j\right)$$

where $x(t_j^+) = \lim_{\eta \to 0^+} x(t_j + \eta)$ with $\eta \in (0, t_{j+1} - t_j)$, and

$$\begin{aligned} \Pi\left(x\left(t_j^+\right), \bar{x}_j\right) =\ & V^*\left(x\left(t_j^+\right)\right) - V^*\left(x(t_j)\right) \\ & + \frac{1}{2} \tilde{\omega}_c^{\mathsf{T}}\left(t_j^+\right) \tilde{\omega}_c\left(t_j^+\right) - \frac{1}{2} \tilde{\omega}_c^{\mathsf{T}}(t_j) \tilde{\omega}_c(t_j). \end{aligned}$$

Suppose that $x(t) \notin E_{c_1} = \{x(t) \in \mathbb{R}^n | \|x(t)\| \leq c_1\}$ or $\tilde{\omega}_c \notin E_{c_2} = \{\tilde{\omega}_c \in \mathbb{R}^n | \left\|\tilde{\omega}_c\right\| \leq c_2\}$. Then, from Situation I, we have $\mathrm{d}L(t)/\mathrm{d}t < 0\ \forall t \in [t_j, t_{j+1})$. That is, $L(t)$ is strictly monotonically decreasing on $[t_j, t_{j+1})$. Thus, it implies

$$L(t_j) > L(t_j + \eta) \quad \forall \eta \in (0, t_{j+1} - t_j). \tag{62}$$

Taking $\eta \to 0^+$ over both sides of (62), we can conclude

$$L\left(t_j\right) \geq \lim_{\eta \to 0^+} L(t_j + \eta) = L\left(t_j^+\right).$$

Thus, we have

$$V^*(x(t_j)) + \frac{1}{2} \tilde{\omega}_c^{\mathsf{T}}(t_j) \tilde{\omega}_c\left(t_j\right) \geq V^*\left(x\left(t_j^+\right)\right) + \frac{1}{2} \tilde{\omega}_c^{\mathsf{T}}\left(t_j^+\right) \tilde{\omega}_c\left(t_j^+\right). \tag{63}$$

From (63), it follows:

$$\Pi\left(x\left(t_j^+\right), \bar{x}_j\right) \leq 0. \tag{64}$$

On the other hand, the uniform ultimate boundedness of the state $x(t)$ in Situation I implies

$$V^*\left(\bar{x}_{j+1}\right) \leq V^*\left(\bar{x}_j\right). \tag{65}$$

Therefore, under the condition that $x(t) \notin E_{c_1} = \{x(t) \in \mathbb{R}^n | \|x(t)\| \leq c_1\}$ (or $\tilde{\omega}_c \notin E_{c_2} = \{\tilde{\omega}_c \in \mathbb{R}^n | \|\tilde{\omega}_c\| \leq c_2\}$), we can conclude that $\Delta L(t_j) < 0$ based on (64) and (65). According to [53], uniform ultimate boundedness of $x(t)$ and $\tilde{\omega}_c$ is guaranteed. Meanwhile, the ultimate bounds of $x(t)$ and $\tilde{\omega}_c$ are c_1 given in (60) and c_2 given in (61), respectively. ■

V. Simulation Study

This section presents two examples to show the effectiveness and applicabilities of the established theoretical results.

A. Example 1: Nonlinear Plants

We study the continuous-time nonlinear system with a mismatched perturbation given by

$$\begin{aligned} \dot{x}_1 &= -x_1 + x_2 + \delta_1 x_1 \cos\left(\frac{1}{x_2 + \delta_2}\right) + \delta_3 x_2 \sin(x_1 x_2) \\ \dot{x}_2 &= -0.5(x_1 + x_2) + 0.5 x_2 \sin^2(x_1) + \sin(x_1) u \end{aligned} \tag{66}$$

where $x = [x_1, x_2]^{\mathsf{T}} \in \mathbb{R}^2$ is the state, $u \in \{u \in \mathbb{R} \colon |u| \leq \beta\}$ is the control input, and $\delta_\varsigma, \varsigma = 1, 2, 3$, are unknown parameters. In this example, we set $\beta = 2$ and randomly choose $\delta_1 \in [-\sqrt{2}/2, \sqrt{2}/2]$, $\delta_2 \in [-100, 100]$, and $\delta_3 \in [-\sqrt{2}/2, \sqrt{2}/2]$. The initial state is $x_0 = [0.5, -0.5]^{\mathsf{T}}$.

The mismatched perturbation in system (66) is

$$d(x) = \delta_1 x_1 \cos\left(\frac{1}{x_2 + \delta_2}\right) + \delta_3 x_2 \sin(x_1 x_2).$$

After making some computations, we obtain $\|d(x)\| \leq \|x\|$. Hence, we can let $d_M(x) = \|x\|$. Since $g(x) = [0, \sin(x_1)]^{\mathsf{T}}$ and $k(x) = [1, 0]^{\mathsf{T}}$, we have $g(x) g^+(x) k(x) = 0$. Then,

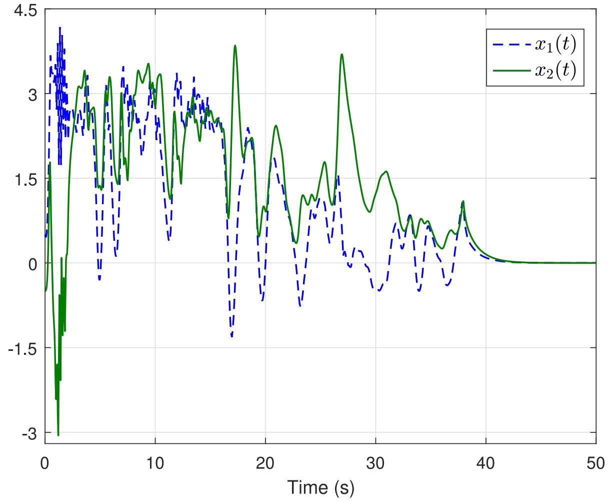

Fig. 2. Evolution of auxiliary system states $x_1(t)$ and $x_2(t)$ in Example 1.

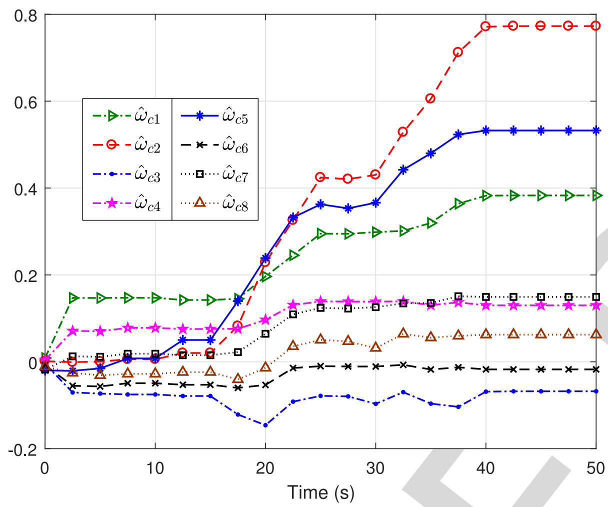

Fig. 3. Convergence of critic network weight vector $\hat{\omega}_c$ in Example 1.

based on (4), the auxiliary system related to (66) can be proposed as

$$\begin{bmatrix}\dot{x}_1\\ \dot{x}_2\end{bmatrix}=\begin{bmatrix}-x_1+x_2\\ -0.5\big(x_1+x_2-x_2\sin^2(x_1)\big)\end{bmatrix}+g(x)u+k(x)\upsilon \tag{67}$$

with $g(x)=[0,\sin(x_1)]^{\mathsf{T}}$, $k(x)=[1,0]^{\mathsf{T}}$, and $\upsilon\in\mathbb{R}$.

Since $\left\|g^{+}(x)k(x)d(x)\right\|=0$, we choose $\ell_M(x)=0$. Let $\rho=0.25$ and $Q=I_2$. Then, based on (5), the cost function for system (67) can be given as

$$V^{u,\upsilon}(x_0)=\int_0^{\infty}\Big(1.25\|x\|^2+\mathcal{W}(u)+0.25\upsilon^{\mathsf{T}}\upsilon\Big)\mathrm{d}t$$

where

$$\begin{aligned}\mathcal{W}(u)&=2\int_0^{u}\beta\tanh^{-1}(\zeta/\beta)\mathrm{d}\zeta\\ &=2\beta u\tanh^{-1}(u/\beta)+\beta^2\ln\Big(1-u^2/\beta^2\Big).\end{aligned}\tag{68}$$

To obtain the optimal ETC, we employ the critic network (34). The parameters used in the critic network and the event-triggering condition (46) are given as follows:

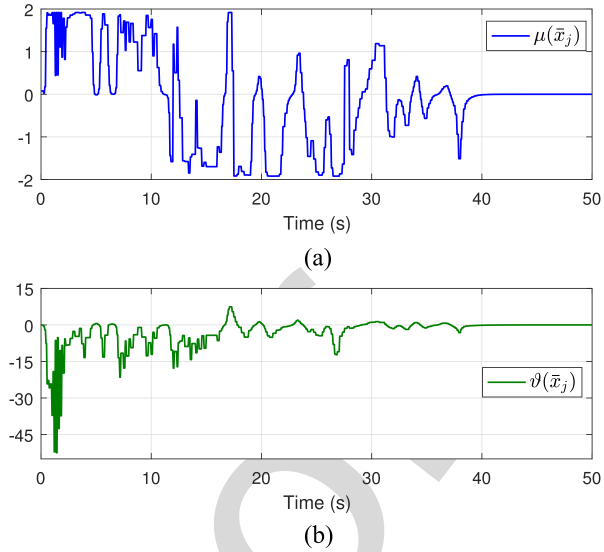

Fig. 4. (a) ETC $\mu(\bar{x}_j)$. (b) Auxiliary ETC $\vartheta(\bar{x}_j)$.

$l_c=0.5$, $\tilde{n}_c=8$, $\gamma=0.3$, and $K_{\max}=3.5$. The basic function vector used in the critic network is

$$\sigma_c(x)=\Big[x_1^2,x_2^2,x_1x_2,x_1^4,x_2^4,x_1^3x_2,x_1^2x_2^2,x_1x_2^3\Big]^{\mathsf{T}}.$$

The weight vector in the critic network is written as $\hat{\omega}_c=[\hat{\omega}_{c1},\hat{\omega}_{c2},\ldots,\hat{\omega}_{c8}]^{\mathsf{T}}$. Furthermore, to ensure φ to be persistently exciting, we add the exploration noise $n_e(t)=12e^{-0.05t}[\sin^2(t)\cos(t)+\sin^2(2t)\cos(0.1t)+\sin^2(-1.2t)\cos(0.5t)+\sin^5(t)+\sin^2(1.12t)+\cos(2.4t)\sin^3(2.4t)]$ into the control at the first 38 s.

Remark 5: Choosing appropriate basic function vectors for critic networks is a challenging issue. Because the number of the elements in the basis function vector is closely associated with the number of neurons in the critic network. In this example, the basic function vector is determined via computer simulations. We find that selecting the basic function vector as the above mentioned $\sigma_c(x)$ can lead to desirable results. In Example 2, the basic function vector is also determined by using computer simulations.

The evolution of auxiliary system states is illustrated in Fig. 2. As displayed in Fig. 2, the auxiliary system states $x_1(t)$ and $x_2(t)$ turn out to be asymptotically stable. The convergence of the critic network weight vector $\hat{\omega}_c$ is shown in Fig. 3. It can be seen that, after the first 40 s, the critic network weight vector converges to $\hat{\omega}_c^{\text{final}}=[0.383,\ 0.773,\ -0.068,\ 0.130,\ 0.533,\ -0.018,\ 0.149,\ 0.062]^{\mathsf{T}}$. Fig. 4(a) and (b) describes the ETC $\mu(\bar{x}_j)$ and the auxiliary ETC $\vartheta(\bar{x}_j)$. The validity of condition (17) is verified by presenting Fig. 5. As indicated in Fig. 5, (17) holds only if $t\geq 40$ s (i.e., $t_s=40$ s). Fig. 6(a) and (b) shows the two norms (i.e., the norm of the event-triggering condition $\|e_j\|$ and the norm of the event-triggering threshold $\|\bar{e}_T\|$) and the sampling period T_s, respectively. Observing Fig. 6(b), we can find that $\min T_s=0.1$ s. Actually, there are 289 state samples in Fig. 6(b), which indicates that only 289 state samples are necessary to implement the ETC algorithm. Nevertheless, under the same

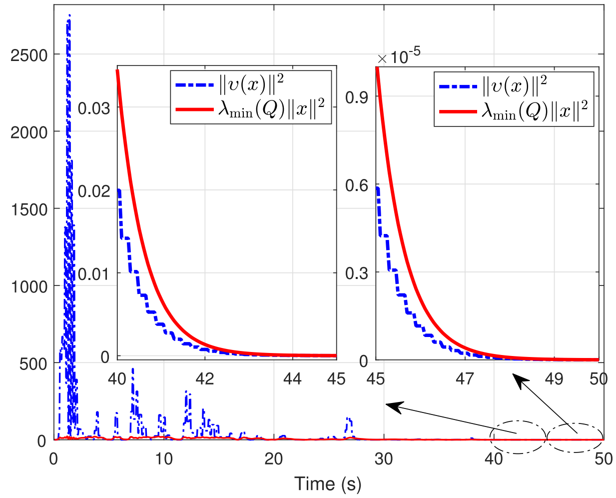

Fig. 5. Verification of condition (17) in Example 1.

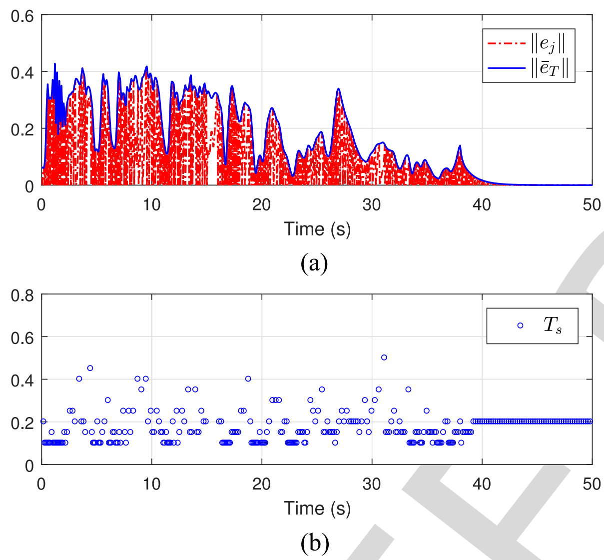

Fig. 6. (a) Norm of the event-triggering condition $\|e_j\|$ and norm of the event-triggering threshold $\|\bar{e}_T\|$. (b) Sampling period T_s in Example 1.

condition, there are 1000 state samples utilized to implement the time-triggering control algorithm. Consequently, the present ETC strategy reduces the controller updates up to 71.1%. In this sense, the computational burden is remarkably decreased. Substituting the above obtained weight vector $\hat{\omega}_c^{\text{final}}$ to (35), we derive the approximate optimal ETC. Fig. 7 displays the states of closed-loop system (66). From Fig. 7, we can see that the states of system (66) are stable under the approximate ETC.

B. Example 2: Application to the Pendulum System

We consider the pendulum system given in [19] as

$$\begin{cases} \frac{d\theta}{dt} &= \nu + d \\ J\frac{d\nu}{dt} &= u - Mgl\sin(\theta) - f_d\frac{d\theta}{dt} \end{cases} \tag{69}$$

with the current angle position of the pendulum $\theta \in \mathbb{R}$, the angular velocity $\nu \in \mathbb{R}$, the perturbation $d \in \mathbb{R}$, the control $u \in \{u \in \mathbb{R}\colon |u| \leq 1\}$ (*note:* $\beta = 1$), the mass of the pendulum

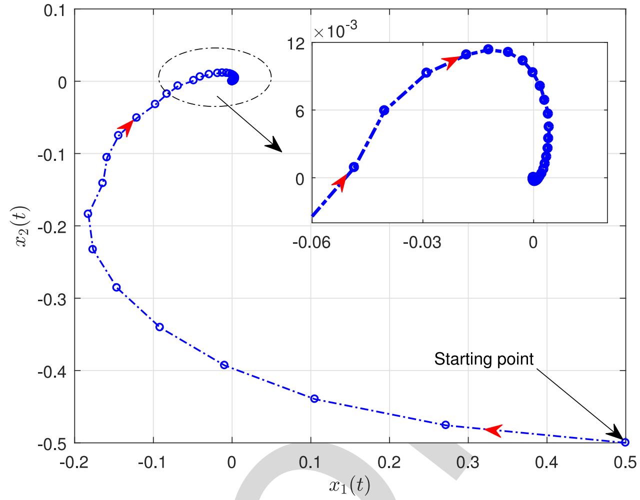

Fig. 7. States $x_1(t)$ and $x_2(t)$ of closed-loop system (66).

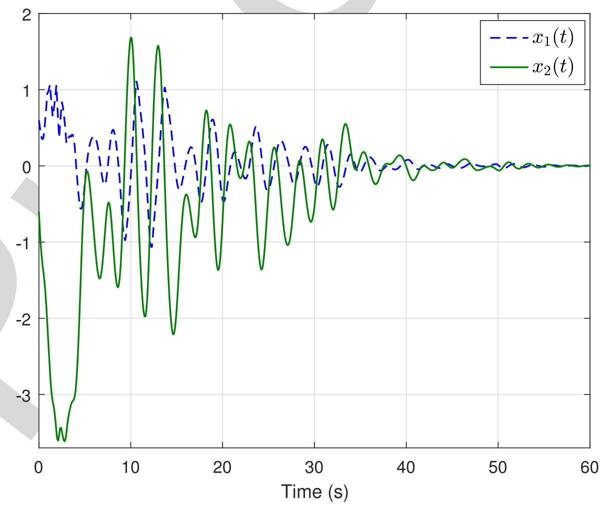

Fig. 8. Evolution of auxiliary system states $x_1(t)$ and $x_2(t)$ in Example 2.

$M = 4/3$ kg, the acceleration of gravity $g = 9.8$ m/s^2, the length of the pendulum $l = 3/2$ m, the rotary inertia $J = 4/3Ml^2$ kg $\cdot$ m^2, and the frictional factor $f_d = 0.2$. We assume that $d = \delta_1\theta\sin(\delta_2\nu)$ with δ_1 and δ_2 randomly chosen within the intervals $[-\sqrt{2}/2, \sqrt{2}/2]$ and $[-2, 2]$, respectively.

Let $x_1 = \theta$ and $x_2 = \nu$. Observing that $g(x) = [0, 0.25]^{\mathsf{T}}$ and $k(x) = [1, -0.2]^{\mathsf{T}}$, we obtain $h(x) = \big(I_2 - g(x)g^{+}(x)\big)k(x) = [1, 0]^{\mathsf{T}}$. Then, according to (4), the auxiliary system related to (69) can be proposed as

$$\begin{bmatrix}\dot{x}_1\\ \dot{x}_2\end{bmatrix} = \begin{bmatrix} x_2 \\ -4.9\sin(x_1) - 0.2x_2\end{bmatrix} + \begin{bmatrix}0\\0.25\end{bmatrix}u + \begin{bmatrix}1\\0\end{bmatrix}\upsilon. \tag{70}$$

The initial state is $x_0 = [0.6, -0.6]^{\mathsf{T}}$. Since $d(x) = \delta_1 x_1\sin(\delta_2 x_2)$, we have that $\|d(x)\| \leq \sqrt{2}/2\|x\|$ and $\big\|g^{+}(x)k(x)d(x)\big\| \leq 0.4\sqrt{2}\|x\|$. Therefore, we choose $d_M(x) = (\sqrt{2}/2)\|x\|$ and $\ell_M(x) = 0.4\sqrt{2}\|x\|$ to satisfy Assumption 2. Selecting $\rho = 0.4$, $Q = I_2$, and using (5), we can present the cost function for system (70) as follows:

$$V^{u,\upsilon}(x_0) = \int_0^{\infty}\Big(1.84\|x\|^2 + \mathcal{W}(u) + 0.4\upsilon^{\mathsf{T}}\upsilon\Big)dt$$

with $\mathcal{W}(u)$ defined as in (68).

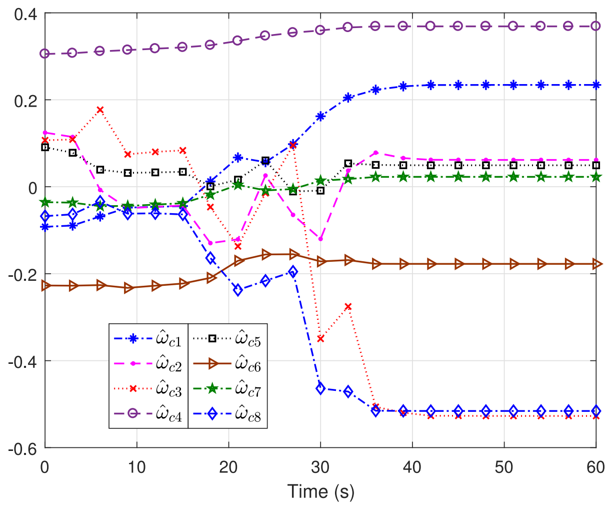

Fig. 9. Convergence of critic network weight vector $\hat{\omega}_c$ in Example 2.

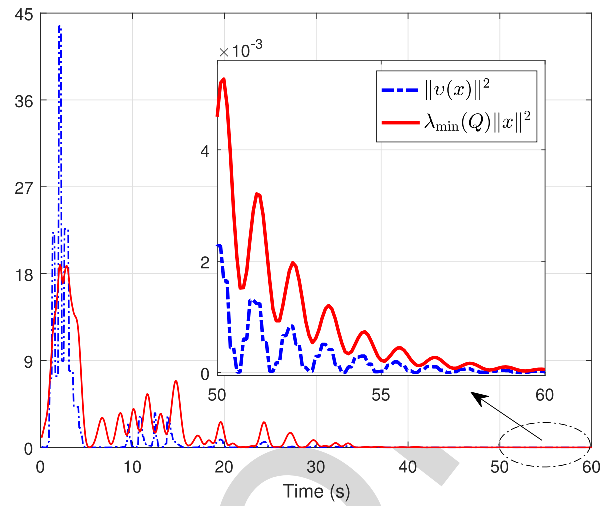

Fig. 11. Verification of condition (17) in Example 2.

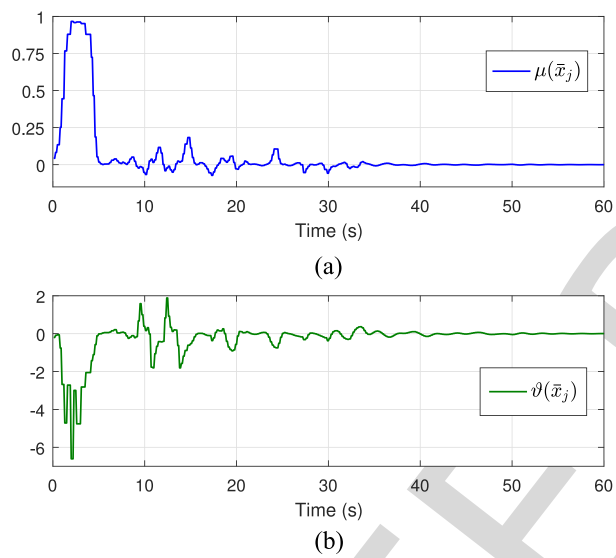

Fig. 10. (a) ETC $\mu(\bar{x}_j)$. (b) Auxiliary ETC $\vartheta(\bar{x}_j)$.

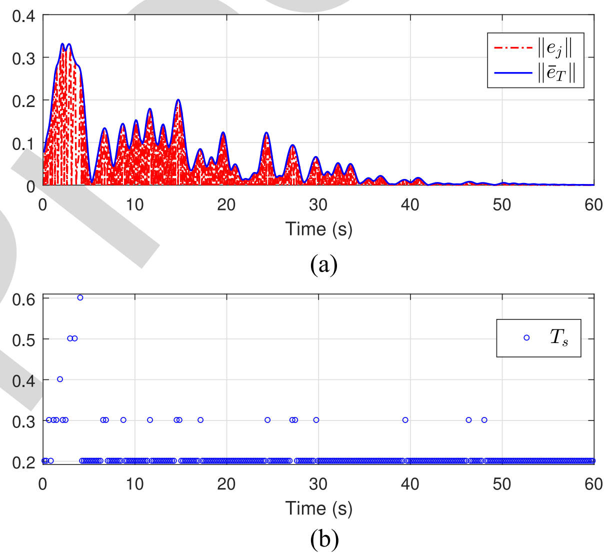

Fig. 12. (a) Norm of the event-triggering condition $\|e_j\|$ and norm of the event-triggering threshold $\|\bar{e}_T\|$. (b) Sampling period T_s in Example 2.

The critic network given as in (34) is applied to derive the optimal ETC law for system (70). The parameters employed in the critic network and the event-triggering condition (46) are the same as in Example 1. The basic function vector used in the critic network is

$$\sigma_c(x) = \left[x_1^2, x_2^2, x_1x_2, x_1^4, x_2^4, x_1^3x_2, x_1^2x_2^2, x_1x_2^3\right]^{\mathsf{T}}$$

and the weight vector in the critic network is denoted as $\hat{\omega}_c = [\hat{\omega}_{c1}, \hat{\omega}_{c2}, \ldots, \hat{\omega}_{c8}]^{\mathsf{T}}$. To ensure φ to be persistently exciting, we add the following exploration noise $n_e(t) = 3e^{-0.15t}[\sin^2(t)\cos(t) + \sin^2(2t)\cos(0.1t) + \sin^2(-1.2t)\cos(0.5t) + \sin^5(t) + \sin^2(1.12t) + \cos(2.4t)\sin^3(2.4t)]$ into the control at the first 50 s.

The evolution of auxiliary system states is displayed in Fig. 8. As illustrated in Fig. 8, the auxiliary system states $x_1(t)$ and $x_2(t)$ are UUB. The convergence of the weight vector $\hat{\omega}_c$ is depicted in Fig. 9. It can be observed that, after the first 50 s, the critic network weight vector converges to $\hat{\omega}_c^{\text{final}} = [0.234, 0.062, -0.527, 0.369, 0.049, -0.177, 0.023, -0.516]^{\mathsf{T}}$. Fig. 10(a) and (b) indicates the ETC $\mu(\bar{x}_j)$ and the auxiliary ETC $\vartheta(\bar{x}_j)$. The validity of condition (17) is verified through Fig. 11. As shown in Fig. 11, (17) holds only if $t \geq 50$ s (i.e., $t_s = 50$ s). Fig. 12(a) and (b) describes the two norms (i.e., the norm of the event-triggering condition $\|e_j\|$ and the norm of the event-triggering threshold $\|\bar{e}_T\|$) and the sampling period T_s, respectively. From Fig. 12(b), we can see that $\min T_s = 0.2$ s. In fact, there are 284 state samples in Fig. 12(b), which shows that only 284 state samples are necessary to implement the ETC algorithm. Nonetheless, under the same condition, there are 600 state samples required to implement the time-triggering control algorithm. Accordingly, the present ETC strategy reduces the controller updates up to 52.67%. In this sense, the computational burden is remarkably decreased. Substituting the above derived weight vector $\hat{\omega}_c^{\text{final}}$ to (35), we obtain the approximate optimal ETC. Fig. 13 displays the states of closed-loop system (69). Observing Fig. 13,

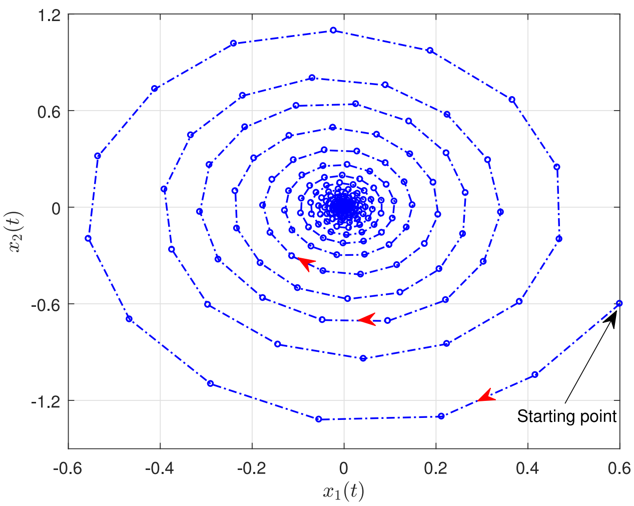

Fig. 13. States $x_1(t)$ and $x_2(t)$ of closed-loop system (69).

we can find that the approximate optimal ETC keeps the states of system (69) stable.

VI. Conclusion

This paper has presented a robust ETC method for nonlinear input-constrained systems with mismatched perturbations. By using an SN-ACD, the robust ETC law was obtained via solving the H_2 optimal control problem. Thus, the proposed control method can avoid the difficulty in judging the existence of saddle points, which arises in H_∞ optimal control problems. However, the developed robust ETC approach has to calculate the Moore–Penrose pseudo-inverse of the control matrix function and offer its upper bounded function. Indeed, this is a limitation when applying the present control strategy to nonlinear systems with complicated structures. Hence, how to relax this condition is one subject of our future studies.

On the other hand, this robust ETC approach is developed for a unique agent system. In recent years, ACDs have been utilized to study optimal regulations of multiagent systems [54], [55]. It is well-known that multiagent plants exist widely in engineering applications, such as the coordination of unmanned aerial vehicles. In addition, packet loss is an important issue arising in multiagent systems, especially networked multiagent systems. Recently, Lu *et al.* [56] proposed an effective model predictive tracking control strategy for networked systems subject to random packet loss and uncertainties. Accordingly, how to extend the SN-ACD to develop robust ETC schemes for multiagent systems with random packet loss and uncertainties is also one direction in our future research.

References

[1] D. V. Prokhorov and D. C. Wunsch, “Adaptive critic designs,” *IEEE Trans. Neural Netw.*, vol. 8, no. 5, pp. 997–1007, Sep. 1997.

[2] D. Wang, D. Liu, Q. Zhang, and D. Zhao, “Data-based adaptive critic designs for nonlinear robust optimal control with uncertain dynamics,” *IEEE Trans. Syst., Man, Cybern., Syst.*, vol. 46, no. 11, pp. 1544–1555, Nov. 2016.

[3] L. Liu, Z. Wang, and H. Zhang, “Neural-network-based robust optimal tracking control for MIMO discrete-time systems with unknown uncertainty using adaptive critic design,” *IEEE Trans. Neural Netw. Learn. Syst.*, vol. 29, no. 4, pp. 1239–1251, Apr. 2018.

[4] D. Liu, Q. Wei, D. Wang, X. Yang, and H. Li, *Adaptive Dynamic Programming With Applications in Optimal Control*. Cham, Switzerland: Springer, 2017.

[5] D. L. Vrabie, K. G. Vamvoudakis, and F. L. Lewis, *Optimal Adaptive Control and Differential Games by Reinforcement Learning Principles*. London, U.K.: IET, 2013.

[6] P. J. Werbos, “Beyond regression: New tools for prediction and analysis in the behavioral sciences,” Ph.D. dissertation, Dept. Appl. Math., Harvard Univ., Cambridge, MA, USA, 1974.

[7] R. S. Sutton and A. G. Barto, *Reinforcement Learning: An Introduction*. Cambridge, MA, USA: MIT Press, 1998.

[8] Q. Wei, F. L. Lewis, D. Liu, R. Song, and H. Lin, “Discrete-time local value iteration adaptive dynamic programming: Convergence analysis,” *IEEE Trans. Syst., Man, Cybern., Syst.*, vol. 48, no. 6, pp. 875–891, Jun. 2018.

[9] Q. Wei, D. Liu, Q. Lin, and R. Song, “Discrete-time optimal control via local policy iteration adaptive dynamic programming,” *IEEE Trans. Cybern.*, vol. 47, no. 10, pp. 3367–3379, Oct. 2017.

[10] X. Zhong, Z. Ni, and H. He, “Gr-GDHP: A new architecture for globalized dual heuristic dynamic programming,” *IEEE Trans. Cybern.*, vol. 47, no. 10, pp. 3318–3330, Oct. 2017.

[11] W. Gao, Y. Jiang, Z.-P. Jiang, and T. Chai, “Output-feedback adaptive optimal control of interconnected systems based on robust adaptive dynamic programming,” *Automatica*, vol. 72, pp. 37–45, Oct. 2016.

[12] Y. Jiang and Z.-P. Jiang, *Robust Adaptive Dynamic Programming*. Hoboken, NJ, USA: Wiley, 2017.

[13] A. Heydari and S. N. Balakrishnan, “Finite-horizon control-constrained nonlinear optimal control using single network adaptive critics,” *IEEE Trans. Neural Netw. Learn. Syst.*, vol. 24, no. 1, pp. 145–157, Jan. 2013.

[14] Z. Wang, L. Liu, H. Zhang, and G. Xiao, “Fault-tolerant controller design for a class of nonlinear MIMO discrete-time systems via online reinforcement learning algorithm,” *IEEE Trans. Syst., Man, Cybern., Syst.*, vol. 46, no. 5, pp. 611–622, May 2016.

[15] V. Narayanan and S. Jagannathan, “Event-triggered distributed control of nonlinear interconnected systems using online reinforcement learning with exploration,” *IEEE Trans. Cybern.*, to be published, doi: 10.1109/TCYB.2017.2741342.

[16] B. Luo, H.-N. Wu, and T. Huang, “Off-policy reinforcement learning for H_∞ control design,” *IEEE Trans. Cybern.*, vol. 45, no. 1, pp. 65–76, Jan. 2015.

[17] X. Xu, Z. Huang, L. Zuo, and H. He, “Manifold-based reinforcement learning via locally linear reconstruction,” *IEEE Trans. Neural Netw. Learn. Syst.*, vol. 28, no. 4, pp. 934–947, Apr. 2017.

[18] B. Luo, T. Huang, H.-N. Wu, and X. Yang, “Data-driven H_∞ control for nonlinear distributed parameter systems,” *IEEE Trans. Neural Netw. Learn. Syst.*, vol. 26, no. 11, pp. 2949–2961, Nov. 2015.

[19] Q. Wei, R. Song, and P. Yan, “Data-driven zero-sum neuro-optimal control for a class of continuous-time unknown nonlinear systems with disturbance using ADP,” *IEEE Trans. Neural Netw. Learn. Syst.*, vol. 27, no. 2, pp. 444–458, Feb. 2016.

[20] H. Jiang, H. Zhang, Y. Luo, and X. Cui, “H_∞ control with constrained input for completely unknown nonlinear systems using data-driven reinforcement learning method,” *Neurocomputing*, vol. 237, pp. 226–234, May 2017.

[21] Y. Zhu, D. Zhao, and X. Li, “Iterative adaptive dynamic programming for solving unknown nonlinear zero-sum game based on online data,” *IEEE Trans. Neural Netw. Learn. Syst.*, vol. 28, no. 3, pp. 714–725, Mar. 2017.

[22] K. G. Vamvoudakis, H. Modares, B. Kiumarsi, and F. L. Lewis, “Game theory-based control system algorithms with real-time reinforcement learning: How to solve multiplayer games online,” *IEEE Control Syst.*, vol. 37, no. 1, pp. 33–52, Feb. 2017.

[23] F. Lin and R. D. Brandt, “An optimal control approach to robust control of robot manipulators,” *IEEE Trans. Robot. Autom.*, vol. 14, no. 1, pp. 69–77, Feb. 1998.

[24] D. M. Adhyaru, I. N. Kar, and M. Gopal, “Bounded robust control of nonlinear systems using neural network–based HJB solution,” *Neural Comput. Appl.*, vol. 20, no. 1, pp. 91–103, Feb. 2011.

[25] C. Mu, C. Sun, D. Wang, and A. Song, “Adaptive tracking control for a class of continuous-time uncertain nonlinear systems using the approximate solution of HJB equation,” *Neurocomputing*, vol. 260, pp. 432–442, Oct. 2017.

[26] Q. Qu, H. Zhang, T. Feng, and H. Jiang, "Decentralized adaptive tracking control scheme for nonlinear large-scale interconnected systems via adaptive dynamic programming," *Neurocomputing*, vol. 225, pp. 1–10, Feb. 2017.

[27] H. Zhang, Q. Qu, G. Xiao, and Y. Cui, "Optimal guaranteed cost sliding mode control for constrained-input nonlinear systems with matched and unmatched disturbances," *IEEE Trans. Neural Netw. Learn. Syst.*, vol. 29, no. 6, pp. 2112–2126, Jun. 2018.

[28] W. P. M. H. Heemels, K. H. Johansson, and P. Tabuada, "An introduction to event-triggered and self-triggered control," in *Proc. 51st IEEE Annu. Conf. Decis. Control*, Maui, HI, USA, Dec. 2012, pp. 3270–3285.

[29] P. Tabuada, "Event-triggered real-time scheduling of stabilizing control tasks," *IEEE Trans. Autom. Control*, vol. 52, no. 9, pp. 1680–1685, Sep. 2007.

[30] K. G. Vamvoudakis, "Event-triggered optimal adaptive control algorithm for continuous-time nonlinear systems," *IEEE/CAA J. Automatica Sinica*, vol. 1, no. 3, pp. 282–293, Jul. 2014.

[31] A. Sahoo, H. Xu, and S. Jagannathan, "Neural network-based event-triggered state feedback control of nonlinear continuous-time systems," *IEEE Trans. Neural Netw. Learn. Syst.*, vol. 27, no. 3, pp. 497–509, Mar. 2016.

[32] A. Sahoo and S. Jagannathan, "Stochastic optimal regulation of nonlinear networked control systems by using event-driven adaptive dynamic programming," *IEEE Trans. Cybern.*, vol. 47, no. 2, pp. 425–438, Feb. 2017.

[33] D. Wang, C. Mu, H. He, and D. Liu, "Event-driven adaptive robust control of nonlinear systems with uncertainties through NDP strategy," *IEEE Trans. Syst., Man, Cybern., Syst.*, vol. 47, no. 7, pp. 1358–1370, Jul. 2017.

[34] Q. Zhang, D. Zhao, and D. Wang, "Event-based robust control for uncertain nonlinear systems using adaptive dynamic programming," *IEEE Trans. Neural Netw. Learn. Syst.*, vol. 29, no. 1, pp. 37–50, Jan. 2018.

[35] C. Mu, D. Wang, C. Sun, and Q. Zong, "Robust adaptive critic control design with network-based event-triggered formulation," *Nonlin. Dyn.*, vol. 90, no. 3, pp. 2023–2035, Nov. 2017.

[36] Q. Zhang, D. Zhao, and Y. Zhu, "Event-triggered H_∞ control for continuous-time nonlinear system via concurrent learning," *IEEE Trans. Syst., Man, Cybern., Syst.*, vol. 47, no. 7, pp. 1071–1081, Jul. 2017.

[37] D. Wang, C. Mu, X. Yang, and D. Liu, "Event-based constrained robust control of affine systems incorporating an adaptive critic mechanism," *IEEE Trans. Syst., Man, Cybern., Syst.*, vol. 47, no. 7, pp. 1602–1612, Jul. 2017.

[38] T. Basar and P. Bernhard, *H_∞ Optimal Control and Related Minimax Design Problems: A Dynamic Game Approach*, 2nd ed. Boston, MA, USA: Birkhäuser, 1995.

[39] K. Sun, Y. Li, and S. Tong, "Fuzzy adaptive output feedback optimal control design for strict-feedback nonlinear systems," *IEEE Trans. Syst., Man, Cybern., Syst.*, vol. 47, no. 1, pp. 33–44, Jan. 2017.

[40] X. Yang and H. He, "Self-learning robust optimal control for continuous-time nonlinear systems with mismatched disturbances," *Neural Netw.*, vol. 99, pp. 19–30, Mar. 2018.

[41] M. Abu-Khalaf, J. Huang, and F. L. Lewis, *Nonlinear H_2/H_∞ Constrained Feedback Control: A Practical Design Approach Using Neural Networks*. London, U.K.: Springer, 2006.

[42] W. Rudin, *Principles of Mathematical Analysis*, 3rd ed. New York, NY, USA: McGraw-Hill, 1976.

[43] X. Yang, H. He, and X. Zhong, "Adaptive dynamic programming for robust regulation and its application to power systems," *IEEE Trans. Ind. Electron.*, vol. 65, no. 7, pp. 5722–5732, Jul. 2018.

[44] W. Liu and J. Huang, "Event-triggered global robust output regulation for a class of nonlinear systems," *IEEE Trans. Autom. Control*, vol. 62, no. 11, pp. 5923–5930, Nov. 2017.

[45] X. Zhong and H. He, "An event-triggered ADP control approach for continuous-time system with unknown internal states," *IEEE Trans. Cybern.*, vol. 47, no. 3, pp. 683–694, Mar. 2017.

[46] D. Liu, X. Yang, D. Wang, and Q. Wei, "Reinforcement-learning-based robust controller design for continuous-time uncertain nonlinear systems subject to input constraints," *IEEE Trans. Cybern.*, vol. 45, no. 7, pp. 1372–1385, Jul. 2015.

[47] F. L. Lewis, S. Jagannathan, and A. Yesildirak, *Neural Network Control of Robot Manipulators and Nonlinear Systems*. London, U.K.: Taylor & Francis, 1999.

[48] M. Heymann, F. Lin, G. Meyer, and S. Resmerita, "Analysis of Zeno behaviors in a class of hybrid systems," *IEEE Trans. Autom. Control*, vol. 50, no. 3, pp. 376–383, Mar. 2005.

[49] Y. Zhu, D. Zhao, H. He, and J. Ji, "Event-triggered optimal control for partially unknown constrained-input systems via adaptive dynamic programming," *IEEE Trans. Ind. Electron.*, vol. 64, no. 5, pp. 4101–4109, May 2017.

[50] D. Wang, H. He, and D. Liu, "Adaptive critic nonlinear robust control: A survey," *IEEE Trans. Cybern.*, vol. 47, no. 10, pp. 3429–3451, Oct. 2017.

[51] B. Igelnik and Y.-H. Pao, "Stochastic choice of basis functions in adaptive function approximation and the functional-link net," *IEEE Trans. Neural Netw.*, vol. 6, no. 6, pp. 1320–1329, Nov. 1995.

[52] K. G. Vamvoudakis, A. Mojoodi, and H. Ferraz, "Event-triggered optimal tracking control of nonlinear systems," *Int. J. Robust Nonlin. Control*, vol. 27, no. 4, pp. 598–619, Mar. 2017.

[53] H. K. Khalil, *Nonlinear Systems*, 3rd ed. Upper Saddle River, NJ, USA: Prentice-Hall, 2002.

[54] H. Zhang, H. Liang, Z. Wang, and T. Feng, "Optimal output regulation for heterogeneous multiagent systems via adaptive dynamic programming," *IEEE Trans. Neural Netw. Learn. Syst.*, vol. 28, no. 1, pp. 18–29, Jan. 2017.

[55] H. Modares, F. L. Lewis, W. Kang, and A. Davoudi, "Optimal synchronization of heterogeneous nonlinear systems with unknown dynamics," *IEEE Trans. Autom. Control*, vol. 63, no. 1, pp. 117–131, Jan. 2018.

[56] R. Lu, Y. Xu, and R. Zhang, "A new design of model predictive tracking control for networked control system under random packet loss and uncertainties," *IEEE Trans. Ind. Electron.*, vol. 63, no. 11, pp. 6999–7007, Nov. 2016.

Xiong Yang received the B.S. degree in mathematics and applied mathematics from Central China Normal University, Wuhan, China, in 2008, the M.S. degree in pure mathematics from Shandong University, Jinan, China, in 2011, and the Ph.D. degree in control theory and control engineering from the Institute of Automation, Chinese Academy of Sciences, Beijing, China, in 2014.

From 2014 to 2016, he was an Assistant Professor with the State Key Laboratory of Management and Control for Complex Systems, Institute of Automation, Chinese Academy of Sciences. Since 2016, he has been a Post-Doctoral Fellow with the Department of Electrical, Computer and Biomedical Engineering, University of Rhode Island, Kingston, RI, USA. He is currently an Associate Professor with the School of Electrical and Information Engineering, Tianjin University, Tianjin, China. His current research interests include adaptive dynamic programming, reinforcement learning, event-triggered control, data-driven control, and their applications.

Dr. Yang was a recipient of the Excellent Award of Presidential Scholarship of the Chinese Academy of Sciences in 2014.

Haibo He (SM'11–F'18) received the B.S. and M.S. degrees in electrical engineering from the Huazhong University of Science and Technology, Wuhan, China, in 1999 and 2002, respectively, and the Ph.D. degree in electrical engineering from Ohio University, Athens, OH, USA, in 2006.

He is currently the Robert Haas Endowed Chair Professor with the Department of Electrical, Computer and Biomedical Engineering, University of Rhode Island, Kingston, RI, USA. He has published one sole-author research book entitled *Self-Adaptive Systems for Machine Intelligence* (Wiley, 2011), edited one book entitled *Imbalanced Learning: Foundations, Algorithms, and Applications* (Wiley-IEEE, 2013) and six conference proceedings (Springer), and authored and coauthored over 300 peer-reviewed journal and conference papers.

Dr. He was the Chair of the IEEE Computational Intelligence Society (CIS) Neural Networks Technical Committee in 2013 and 2014 and the IEEE CIS Emergent Technologies Technical Committee in 2015. He was the General Chair of the IEEE Symposium Series on Computational Intelligence in 2014. He was a recipient of the IEEE International Conference on Communications Best Paper Award in 2014, the IEEE CIS Outstanding Early Career Award in 2014, the U.S. National Science Foundation CAREER Award in 2011, and the Providence Business News "Rising Star Innovator" Award in 2011. He is currently the Editor-in-Chief of the IEEE TRANSACTIONS ON NEURAL NETWORKS AND LEARNING SYSTEMS.